Rare codon differences affect expression of the neurodevelopmental protein paralogs NDE1 and NDEL1

Kršanac, Matea

Master's thesis / Diplomski rad

2023

Degree Grantor / Ustanova koja je dodijelila akademski / stručni stupanj: **University of Rijeka / Sveučilište u Rijeci**

Permanent link / Trajna poveznica: https://urn.nsk.hr/urn:nbn:hr:193:006846

Rights / Prava: In copyright/Zaštićeno autorskim pravom.

Download date / Datum preuzimanja: **2025-01-12**

Repository / Repozitorij:

Repository of the University of Rijeka, Faculty of Biotechnology and Drug Development - BIOTECHRI Repository

UNIVERSITY OF RIJEKA

DEPARTMENT OF BIOTECHOLOGY

Graduate university programme

"Biotechnology in Medicine"

Matea Kršanac

Rare codon differences affect expression of the neurodevelopmental protein paralogs NDE1 and NDEL1

Master's thesis

Rijeka, 2023

UNIVERSITY OF RIJEKA

DEPARTMENT OF BIOTECHOLOGY

Graduate university programme

"Biotechnology in medicine"

Matea Kršanac

Rare codon differences affect expression of the neurodevelopmental protein paralogs NDE1 and NDEL1

Master's thesis

Rijeka, 2023

Mentor: Nicholas J. Bradshaw, PhD

SVEUČILIŠTE U RIJECI

ODJEL ZA BIOTEHNOLOGIJU

Diplomski sveuličišni studij

"Biotehnologija u medicini"

Matea Kršanac

Razlike u rijetkim kodonima utječu na ekspresiju neurorazvojnih proteinskih paraloga NDE1 i NDEL1

Diplomski rad

Rijeka, 2023

Mentor rada: izv. prof. dr. sc. Nicholas J. Bradshaw

Master's thesis was defended on 27th September 2023.

In front of the Committee:

1. prof. dr. sc. Miranda Mladinić Pejatović

2. prof. dr. sc. Mladen Merćep

3. izv. prof. dr. sc. Nicholas J. Bradshaw

This thesis has 76 pages, 16 figures, 10 tables and 85 citations.

Abstract

Chronic mental illnesses are persistent and disrupt cognition, emotion regulation and behaviour, and their exact causes and mechanisms remain largely unknown. Previous studies identified several genetic factors that play a role in their development. Nuclear Distribution Element 1 (NDE1) and Nuclear Distribution Element-Like 1 (NDEL1) are proteins that arise form a gene duplication event and are vital in cell mitosis and neurodevelopment. They have been associated with brain malformations and neurodevelopmental disorders. Although being structurally similar, they exhibit distinct pathophysiological functions.

Rare codon bias is a tendency for some codons to be more frequently used than others in a specific species, while they encode for the same amino acid. Codon rarity has been demonstrated to affect translation speed, protein folding, translational control, and protein expression levels in multiple known genomes. In human *NDE1* and *NDEL1* genes, the latter shows an increase in frequency of rare codon usage.

In this thesis, I first investigated whether the difference in codon rarity between *NDE1* and *NDEL1* was conserved across multiple species that represented major vertebrate genera. Next, I explored if altering the codons responsible for encoding NDE1 and NDEL1 could mitigate the differences in expression levels between these two proteins. To achieve this, I examined NDE1 constructs that used codons closely, matching ones found in NDEL1, while maintaining the correct amino acid sequence, and vice versa. Finally, I examined the expression patterns of both wild type and switched codon NDE1 and NDEL1 proteins by fluorescent microscopy with the aim of identifying any noticeable distinctions if such differences existed.

The preference of *NDEL1* for rare codon usage that had previously been seen in humans, was also seen in non-human primates and non-primate mammals,

suggesting the rare codon bias differences between the two genes to be conserved across mammalian species. Our findings indicated that the difference in codon rarity in wild type NDE1 and NDEL1 had an impact on their respective expression levels, with NDE1 exhibiting higher expression within cells. Notably, when examining constructs with switched codons, there was indication of this difference being nullified. This observation suggests that the use of more commonly occurring codons could potentially reverse the trend of lower protein expression levels and that rare codon bias may be partially responsible for the differing functions of the two proteins.

Sažetak

Kronične mentalne bolesti su dugotrajne i ometaju kogniciju, regulaciju emocija i ponašanje, a njihovi točni uzroci i mehanizmi uglavnom su nepoznati. Prethodne studije identificirale su nekoliko gena koji igraju ulogu u njihovom razvoju. Nuklearni distribucijski element 1 (NDE1) i nuklearni distribucijski element sličan 1 (NDEL1) su proteini nastali duplikacijom gena koji sudjeluju u staničnoj mitozi i neurološkom razvoju te su povezani s malformacijama mozga i neurološkim poremećajima. Iako su strukturno slični, njihove se patofiziološke funkcije značajno razlikuju.

Pristranost rijetkim kodonima je tendencija da se neki kodon koristi češće od drugih u određenoj vrsti, kada je riječ o onima koji kodiraju istu aminokiselinu. Kod ljudi, *NDEL1* gen pokazuje veću učestalost korištenja rijetkih kodona u odnosu na *NDE1* gen. Pokazalo se da rijetkost kodona utječe na brzinu translacije, savijanje proteina, kontrolu translacije i razine ekspresije proteina u većem broju istraženih genoma.

U diplomskom radu najprije sam istražila je li razlika u rijetkosti kodona između NDE1 i NDEL1 očuvana u više reprezentativnih vrsta rodova kralješnjaka. Zatim sam istražila može li zamjena kodona odgovornih za kodiranje NDE1 i NDEL1 ublažiti razlike u razinama ekspresije između ova dva proteina. U tu svrhu ispitivala sam NDE1 konstrukte kodirane kodonima bliskim onima koje koristi NDEL1 uz očuvanje točne aminokiselinske sekvence, i obrnuto. Na kraju sam fluorescentnom mikroskopijom ispitala gdje se unutar stanica eksprimiraju NDE1 i NDEL1 proteini divljeg tipa i onih s promijenjenim kodonima kako bi utvrdili postoje li očite razlike.

Pristranost za rijetke kodone kod NDEL1 ranije je uočena kod ljudi, a sada i kod primata i sisavaca koji nisu primati, što ukazuje da je razlika u pristranosti evolucijski očuvana u sisavcima. Naši rezultati pokazali su da je razlika u rijetkosti kodona u divljem tipu NDE1 i NDEL1 imala utjecaj na njihovu razinu

ekspresije, pri čemu NDE1 pokazuje veću ekspresiju unutar stanica. Pri ispitivanju konstrukata sa zamijenjenim kodonima, postojala je indikacija da je ova razlika u ekspresiji poništena. Ovo opažanje sugerira da bi korištenje kodona koji se češće pojavljuju moglo potencijalno preokrenuti trend nižih razina ekspresije proteina, te da bi pristranost za rijetke kodone mogla biti djelomično odgovorna za različite funkcije dvaju proteina.

Ključne riječi: kronična mentalna bolest, NDE1, NDEL1, pristranost rijetkim kodonima, ekspresija proteina

Acknowledgements

I wish to express my sincere gratitude to my mentor, Nicholas J. Bradshaw, for the incredible opportunity to learn and grow under his expert guidance over the past few months. He was always available for any questions and doubts, allowing me to gain a valuable experience working in the lab.

I want to extend my gratitude to Beti and Bobana, who helped teach me new techniques and guided me throughout the making of this thesis. Thank you for giving me support and helping me not give up when things were not going as planned. Your company not only eased those moments but also transformed them into pleasant and delightful experiences.

Special thanks to my lab mates, Ema, and Lana, with whom I shared numerous enjoyable moments during the extensive waits accompanying our experiments.

Thank you to my family for supporting me throughout my studies and giving me countless opportunities to do the things I enjoy most.

Finally, I want to extend a heartfelt thank you to my partner. Your belief in my abilities and your support through all the ups and downs of this journey have been irreplaceable. Your encouragement has been an essential part of my success, and I am truly grateful for your presence in my life.

Table of contents

List of abbreviations

AAA	ATPases Associated with Diverse Cellular Activities
CENP-F	Centromere Protein F
DHC	Dynein Heavy Chain
DIC	Dynein Intermediate Chain
DISC1	Disrupted in Schizophrenia 1
DSM-5	Diagnostic and Statistical Manual of Mental Disorders (5th edition)
KATNA1	Katanin Catalytic Subunit A1
KATNB1	Katanin Regulatory Subunit B1
LC8	Dynein Light Chain 8
LIS1	Lissencephaly 1
NDE1	Nuclear Distribution Element 1
NDE1-NLc	NDE1 protein with NDEL1-like codons
NDE1-WT	Wild type NDE1
NDEL1	Nuclear Distribution Element-Like 1
NDEL1-Nc	NDEL1 protein with NDE1-like codons
NDEL1-WT	Wild type NDEL1 protein
NF-H	Neurofilament Heavy Chain
NF-L	Neurofilament Light Chain

1. Introduction

1.1. Chronic mental illness

Chronic mental illnesses are long lasting and reoccurring clinically significant disruptions in an individual's cognition, emotional regulation, or behaviour (1,2). According to the World Health Organization (WHO), 970 million people worldwide were living with a mental illness in 2019, representing a 25% increase in prevalence since 2000. Anxiety and depressive type disorders stand out as the two most prevalent subtypes, exhibiting variations in sex and age.

A consensus on the fundamental dimensions within the definition of chronic mental illness includes three main criteria: diagnostic criteria, illness duration and disability criteria (3,4). Diagnostic guidelines can be found in two main sources, the fifth edition of the Diagnostic and Statistical Manual of Mental Disorders (DSM-5) or in the eleventh revision of the International Classification of Diseases and Related Health Problems (ICD-11) (5,6). Both resources categorize disorders into multiple categories based on common characteristics. The disability criterion includes disruptive behaviours that affect day-to-day activities, as well as slight impairment of basic needs (4).

Although major advancements have been made in the understanding of the cause for mental illness development, specific causes and mechanisms remain elusive. Family, twin, adoption and, more recently, genome-wide association studies resulted in the identification of genetic risk factors for multiple clinically diagnosed disorders or severe expression of some psychiatric traits (7). Despite many of these genes and genetic variants being shared between different disorders, these studies represent promising starting points for further research.

1.2. Nuclear Distribution Element 1 and Nuclear Distribution Element-Like 1

Nuclear Distribution Element 1 (NDE1, also known as NUDE) and Nuclear Distribution Element-like 1 (NDEL1, also known as NUDEL) are highly similar members of the nudE protein family that are fundamental for cell mitosis and neurodevelopment (8–10). Originating from a common ancestral gene, these paralogs appear to have distinct pathophysiological roles despite sharing approximately 50% amino acid sequence identity with each other (9,11). Both NDE1 and NDEL1 have been known to interact with cytoplasmic dynein 1 and lissencephaly 1 protein (LIS1) (12,13), however, the mechanism through which they act remains uncertain (9,11). Biallelic mutations, deletions and copy number variations affecting the 16p13.11 chromosomal locus, which contains the *NDE1* gene, have been associated with severe brain malformations and neurodevelopmental disorders like autism and intellectual disability (14–19). Disease association has not been as well characterized for *NDEL1* located at chromosomal position 17p13.1, likely because substantial mutations in the gene interfere with viable development. Previous studies showed targeted *Ndel1* knockout in mice is lethal shortly after embryonic implantation (10,11). Conversely, *Nde1* knockout in mice produces neurodevelopmental abnormalities reminiscent of lissencephaly, such as a thinner cortex and reduced number of cortical neurons. Furthermore, similar results have been documented in humans with *NDE1* mutations that have been shown to cause lissencephaly or microcephaly.

1.2.1. *NDE1* and *NDEL1* evolution

NDE1 and *NDEL1* arise from a gene duplication event, which corresponds to the time when vertebrates developed (Figure 1) (17,20). Previous phylogenetic analyses showed that invertebrates contain a single gene equivalent to *NDE1* and *NDEL1*, which cannot be identified as exclusively corresponding to either (21). Conversely, vertebrates have a clear distinction between sets of *NDE1* and *NDEL1* proteins that have evolved along two

2

different paths following the gene duplication event. It is likely that these separate evolutionary trajectories led the proteins to adopt distinct functionalities. Interestingly, studies on zebrafish revealed the existence of two *NDEL1* orthologs, suggesting that an extra duplication process contributed to the further division of functions (22). While it is only published for zebrafish, it is likely that this division is conserved among other fish species.
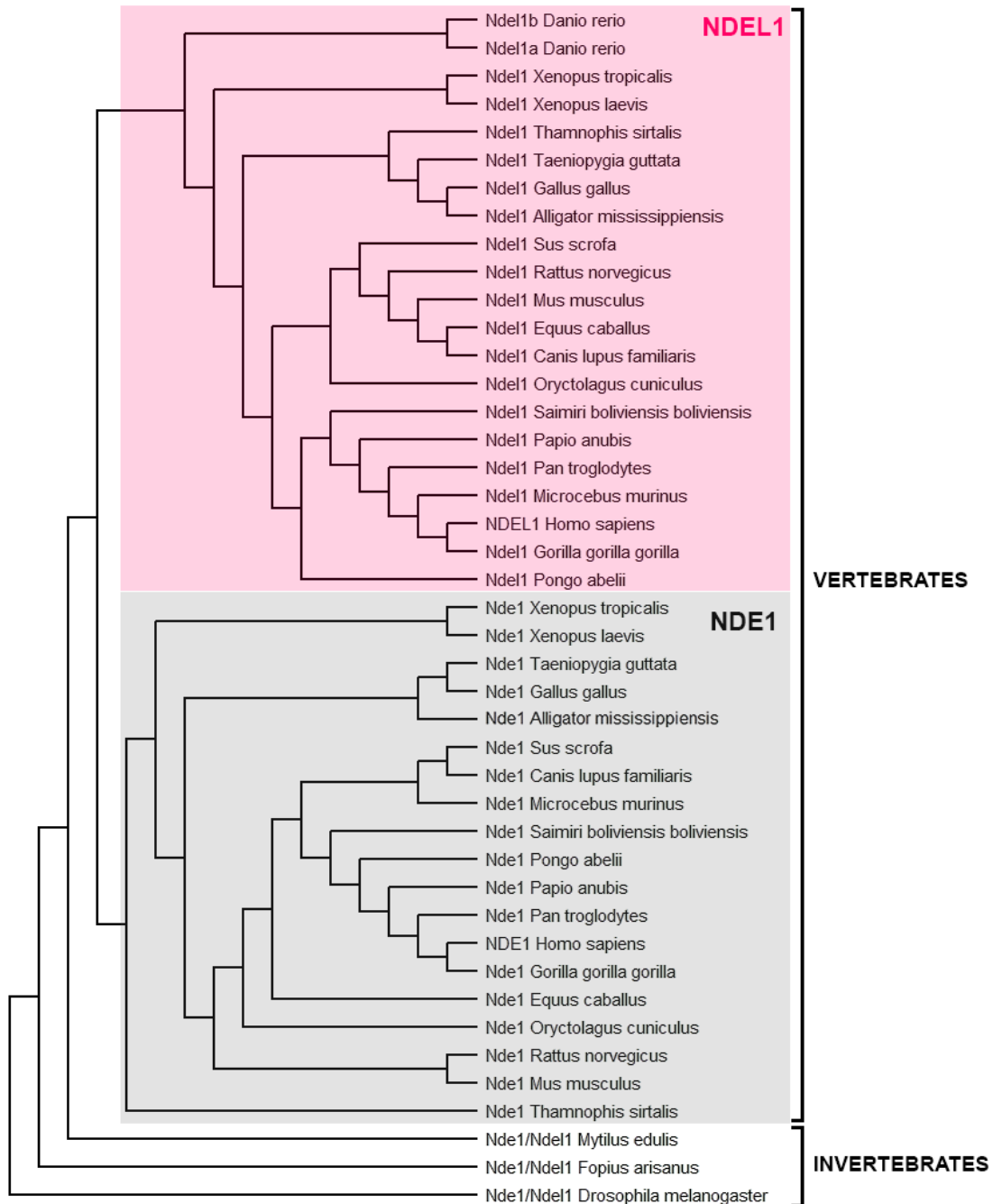
Figure 1. **Phylogenetic tree of Nde1 and Ndel1 protein sequences.** In agreement with previous research, NDE1 (marked in grey) and NDEL1 (marked in pink) seem to arise from a gene duplication event corresponding to vertebrate development. Individual sequences for each species were retrieved from the UCSC Genome Browser (www.genome-euro.ucsc.edu) or UniProt (www.uniprot.org) (23,24). Sequence alignment was performed using the MUSCLE algorithm available

in the Molecular Evolutionary Genetics Analysis (MEGA) software (www.megasoftware.net), which was also used to generate the phylogenetic tree (25). Vertebrate and invertebrate species are marked with respective brackets.

1.2.2. Protein domains and structure

NDE1 and NDEL1 share similar lengths as proteins, with their major isoforms consisting of 335 and 345 amino acid residues, respectively (8,9,11). Analysing their amino acid sequences reveals a high degree of conservation, primarily found at the N-terminal region, while the C-terminal sequence is more variable (Figure 2). Although a full-length three-dimensional structure of the paralogs is not yet available, previous structure-based work focused solely on NDEL1 unveiled specific features.
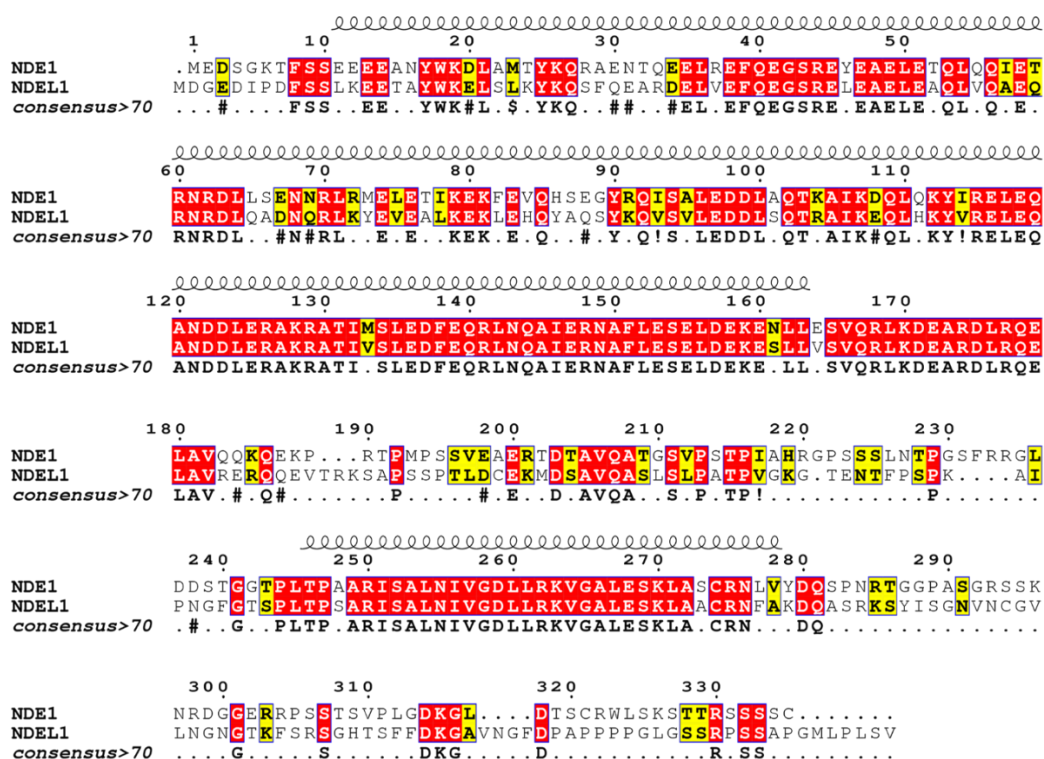
Figure 2. **Human NDE1 and NDEL1 sequence alignment.** Sequences of human NDE1 and NDEL1 were obtained using the UCSC Genome Browser (www.genome-euro.ucsc.edu) (23) with accession numbers NM_017668 and NM_030808,

respectively. The location of the N-terminal coiled-coil domain (residues 10-185) (9,20) and the predicted C-terminal α-helix (residues 247–278) (11,20) is indicated above the aligned sequences. Conserved residues are highlighted in red, while residues that were conservatively substituted are highlighted in yellow. The generated consensus sequence is shown below the alignment (strictly conserved amino acids are marked with uppercase letters; lowercase letters indicate a consensus level >0.5; ! is consensus I or V; $ for L or M; % for F or Y; and # for N, D, Q, B). Sequences were aligned using Clustal Omega (26), and the figure was generated with ESPript v3.0 (www.espript.ibcp.fr) (27).

The N-terminal region of NDEL1 contains an N-terminal coiled-coil domain spanning residues 10-185, which has been confirmed by crystallography studies (Figure 3B) (9,20). This domain is involved in protein dimerization in which two identical monomeric NDEL1 species, each a continuous α-helix, form a parallel coiled structure. Additionally, dimerized NDEL1 fragments (residues 8-167) interacted with another dimer in a tail-to-tail manner to form antiparallel homotetramers. These findings were supported by further research involving mass spectroscopy and chemical cross-linking, where NDEL1 formed parallel dimers in solution (8,20). Furthermore, the full-length protein has been seen to form extended "needle-like" arrangements in solution (Figure 3D), consistent with previously seen crystal structures. Full-length NDE1 also exhibited "needle-like" dimers and tetramers in solution, suggesting the structure of the coiled-coil domain to be conserved in both proteins. This conservation was expected, given the high level of amino acid sequence similarity within those specific residues.

Derewenda et al. further examined the coiled-coil structure and identified three separate regions (Figure 3C) (9). Regions I and II, spanning residues 10-37 and 40-99, respectively, form a highly stable parallel dimer and are separated with a three-residue insertion. They adhere to a classical 3:4

hydrophobic heptad repeat, pattern, in which the first and fourth residue are of hydrophobic nature (9,28). Both regions maintain an α-helical structure and contain five and seven heptad repeats, respectively. Region III, containing residues 100-166, retains the α-helical structure, but is unstable in nature. Interestingly, crystallography analyses showed region III to be involved in forming antiparallel four-helix bundles between two NDEL1 dimers.

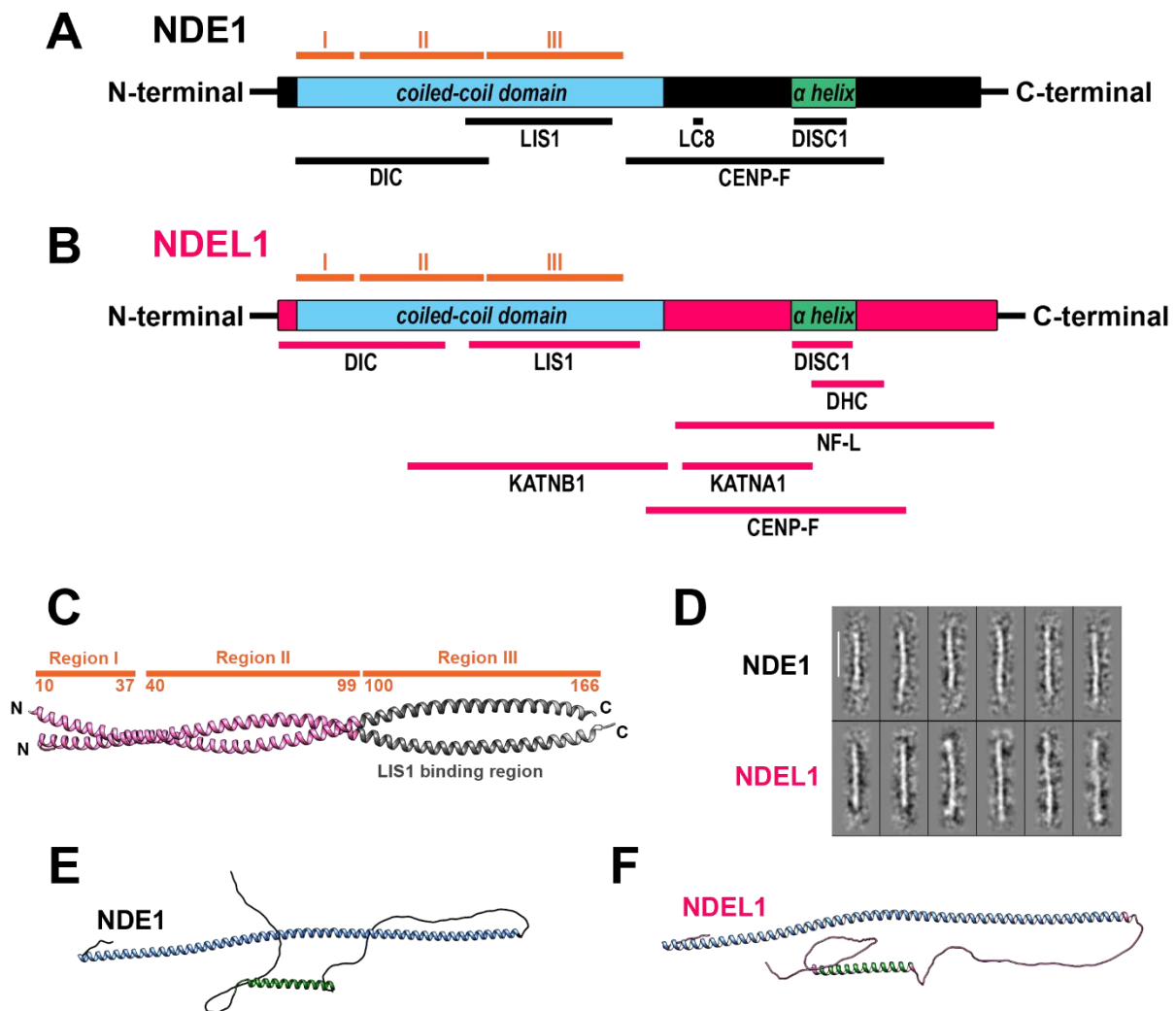Figure 3. **Protein domain architecture and structure of human NDE1 and NDEL1.** (A) Schematic representation of NDE1 (in black) protein structure and domains drawn to scale. N-terminal coiled-coil domain (residues 10-185) (9,20) and the predicted C-terminal α-helix (residues 247–278) (11,20) are marked in blue and green, respectively. Regions I, II and III within the coiled-coil domain are labelled in

orange. NDE1 interactor binding sites are represented below the structure with black lines drawn to scale. Binding site residues for interactors are found in literature: DIC (11,29), LIS1 (30), LC8 (11), DISC1 (31), CENP-F (32). (B) Schematic representation of NDEL1 (in pink) protein structure and domains drawn to scale. N-terminal coiled-coil domain (residues 10-185) (9,20) and the predicted C-terminal α-helix (residues 247–278) (11,20) are marked in blue and green, respectively. Regions I, II and III within the coiled-coil domain are labelled in orange. NDEL1 interactor binding sites are represented below the structure with pink lines drawn to scale. Binding site residues for interactors are found in literature: DIC (33), LIS1 (11), DISC1 (31), DHC (11), NF-L (34), KATNB1 (35,36), KATNA1 (36), CENP-F (37). (C) View of the coiled-coil domain structure of NDEL1 fragment (residues 8-167) with labelled regions I, II and III. The dimer consists of two NDEL1 fragment monomers (in pink). LIS1 binding region (residues 85-169) (11) is shown in grey. (D) Electron microscopy of NDE1 (top row) and NDEL1 (bottom row) proteins that show a "needle-like" structure Scale bar is shown in white and represents 20nm. Image adapted from Soares et al. (8) (E,F) Predicted three-dimensional structure of NDE1 and NDEL1. N-terminal coiled-coil domain is shown in blue, and the predicted C-terminal α-helix in green. Structures obtained from Alphafold (AF-Q9NXR1-F1, AF-Q9GZM8-F1) (38,39) and analysed in UCSF Chimera (40).

A flexible disordered linked region is found downstream of the coiled-coil domain, spanning residues 186-247 (11,20). This proline-rich linker region allows the protein to take up a "bent-back" conformation, allowing the interaction between the N-terminal coiled-coil and C-terminal regions (8). Residues 247-278 contain a strongly predicted α-helical structure that interacts with the N-terminal region of the protein and overlaps with the binding site of some interaction partners (8,11,20,41). Notably, this region is highly conserved in sequence identity between NDE1 and NDEL1. Another disordered region is present at the extreme C-terminal end of the protein, which has demonstrated the ability to cross-link two monomers when the

protein forms dimeric structures in solution. Furthermore, this region includes binding sites for several other interaction partners that allow the protein to perform its function.

1.2.3. Post-translational modifications

Although similar in structure, NDE1 and NDEL1 are subject to post-translational modifications that differ to a certain degree between the proteins, likely causing the different functional outcomes (11,20). NDE1 and NDEL1 are highly phosphorylated by an array of kinases, affecting protein localization and interaction with its binding partners. Over thirty phosphorylation sites have been identified, many that are localized to the disordered region between the two coiled domains. Post-translational modifications on this linker region are likely facilitating its ability to form the "bent-back" structure, as well as modulating the interaction of the paralogs with their binding partners (20). As the sites in this region are located next to proline residues, they are targets of proline-directed kinases, such as Cdk1, Cdk5, Erk2, GSK-3 and MAPK. Cdk1 phosphorylation of NDE1 triggers its localization to kinetochores, while Cdk5 and Erk2 phosphorylation of NDEL1 have been shown to increase its binding affinity for dynein, and successful association with lissencephaly 1, respectively (11).

The C-terminal region, more precisely the disordered region spanning from residues 278 to the end of the protein, is another part of the protein that contains a higher number of phosphorylation sites (20). These are mostly targeted by basophilic kinases, including protein kinase A (PKA) and protein kinase C (PKC). PKA phosphorylation of NDE1 can occur at multiple sites, one of which is Ser306, which is not conserved in NDEL1 (11,20,42). Due to its proximity to binding sites for NDE1 interactors, the site is believed to influence protein interactions through phosphorylation. Subsequent studies identified Thr131 in NDE1, conserved in NDEL1 as Thr132, as another noteworthy PKA phosphorylation site. This process is mediated by phosphodiesterase-4 (PDE4)

and disrupted in schizophrenia 1 (DISC1) (42). Introducing a phosphomimic mutation to Thr131 in NDE1 impacted both LIS1 binding affinity and the process of heterodimerization and tetramerization with NDEL1. This suggests that PKA-mediated phosphorylation and subsequent dephosphorylation act as a switch, determining whether NDE1 exhibits a preference for binding with LIS1 or NDEL1.

1.2.4. NDE1 and NDEL1 association with disorders

1.2.4.1. Lissencephaly

The platelet-activating factor acetylhydrolase isoform 1b regulatory subunit 1 (*PAFAH1B1*) gene, also known as lissencephaly 1 (*LIS1*), encodes for a developmentally critical protein first discovered for its involvement in a neuronal migration disorder (43–45). LIS1 protein is expressed in a wide array of tissues and during multiple developmental stages, and its depletion impairs proper neuronal positioning in cerebral cortex layers. Haploinsufficiency of the gene has been linked to lissencephaly, a malformation of the cerebral cortex.

After being identified as a NDE1 and NDEL1 interaction partner, the LIS1 binding site has been mapped on the paralogs. The binding site for LIS1 was first identified on NDEL1, when its N-terminal-coiled-coil domain structure was shown by crystallography (9). Later studies characterised the interaction as relatively strong, and the binding site was additionally mapped to NDE1 with high precision (11,33). The site is found in the coiled-coil domain, spanning residues 90-159 and 85-169 for NDE1 and NDEL1 (Figure 3A, Figure 3B), respectively (11,30).

The term "lissencephaly", meaning "smooth brain" in Ancient Greek, comprises of a heterogenous spectrum of severe brain malformations, which can be divided in two main categories: classic or type I lissencephaly and cobblestone or type II lissencephaly (46,47). Cobblestone lissencephalies

represent the more severe end of the spectrum, as they are often seen as a part of a multisystem disorder, with compromised integrity of the pial surface. The key distinguishing feature of classical lissencephaly is the presence of an abnormally thick cortex with absent or reduced cerebral convulsions (48,49). Many genes have been implied in various lissencephaly sub-types, including *LIS1*. This gene has been associated with two clinical phenotypes of classic lissencephaly: Miller-Diekers syndrome (MDS) and isolated lissencephaly sequence (ILS) (46). Miller-Diekers syndrome can be distinguished from ILS by the presence of distinct facial features, such as a prominent forehead, short nose, protuberant upper lip, and a small jaw. On the other hand, ILS includes only classical lissencephaly, and is caused by small mutations and deletions of the LIS1 gene. Additional features of MDS are caused by much larger deletions, which include neighbouring *LIS1* genes. As the *LIS1* gene is located at the 17p13.3 chromosomal position, one of its neighbouring genes is *NDEL1*, and these two proteins have been shown to interact, giving the basis of NDEL1 involvement in lissencephaly type disorders.

As previously mentioned, severe *NDEL1* mutations have been shown to be more challenging to study, as animal knockout models were not viable. However, the paralog gene, *NDE1* has been studied and linked to some lissencephaly forms. Homozygous mutations of the gene have been shown as causes of microlissencephaly, a type of lissencephaly that is associated with a head circumference at birth of less than three standard deviations below the mean (49). More specifically, these mutations are localized to the C-terminal domain of NDE1, which is identified to contain several binding sites for other interactors. Other features of microlissencephaly include a proportionate reduction of cerebellum and brain stem size, agenesis of the corpus callosum

that connects left and right brain hemispheres, as well as poor overall growth seen in patients (18,49).

1.2.4.2. Schizophrenia

Schizophrenia is a severe psychotic disorder that involves a range of cognitive, behavioural, and emotional dysfunctions (6,50). Affecting around 1% of the worldwide population (51,52), its symptoms commonly emerge between late teen years and late twenties. As outlined in the DSM-5, the criteria for formal schizophrenia diagnosis require two or more symptoms to persist during a significant portion of time in a one-month period (6). These symptoms include delusions, hallucinations, disorganized speech, disorganized or catatonic behaviour, or negative symptoms such as avolition or anhedonia. Additional features supporting the diagnosis can include disturbed sleep patterns, depersonalization, derealisation, abnormalities in sensory processing, attention impairment and cognitive deficits.

Like many other common disorders, there are multiple factors contributing to the onset of schizophrenia, including genetic, epigenetic, stochastic, and environmental factors (14). An array of family, twin and adoption studies identified several genetic factors that play a role in its development. Notably, disrupted in schizophrenia 1 (DISC1) has been identified as a genetic risk factor linked to schizophrenia, as well as several other mental disorders like bipolar disorder, major depressive disorder, and autism spectrum disorders (14,41).

Although the mechanism by which DISC1 impacts neurocognitive function and development remains elusive, numerous proteins have been reported as its interactors (31). Among these, NDE1 and NDEL1 are known binding partners of DISC1, and their interaction has been shown as critical to several neurodevelopmental processes that are abnormal in schizophrenia (53). Both

paralogs interact with DISC1 with their predicted C-terminal α-helical structure (Figure 3A, Figure 3B) (31).

NDE1 has been recognized as a potential susceptibility site for schizophrenia due to its interaction with DISC1, chromosomal location and role in neurodevelopment. Recent studies focused on how NDE1 might affect disease development by identifying rare mutations and how they contribute to schizophrenia (54,55). Kimura et al. identified three novel missense mutations in schizophrenia samples, all located in the disordered NDE1 region between the N-terminal coiled-coil and predicted α-helix (54). Interestingly, this flexible region contains many phosphorylation sites, which are likely impacting the proteins' structure and interactions. Burdick et al. reported a four-locus haplotype of NDEL1 that is associated with increased risk of schizophrenia (53). Furthermore, preliminary evidence of epistatic interactions between a functional DISC1 polymorphism (Ser704Cys) and variations in NDEL1 were found. These variations have been seen to impact schizophrenia susceptibility.

1.2.5. Cellular functions of NDE1 and NDEL1

Over the years, numerous interaction partners facilitating the functions of NDE1 and NDEL1 have been uncovered (11,17,20). However, the exact molecular mechanisms of action remain elusive. NDE1 and NDEL1 were first identified as members of the network of regulatory proteins that mediate the actions of the motor protein cytoplasmic dynein 1. Another member of the dynein regulatory network is the protein LIS1, and when forming a complex with the paralogs, they impact mitotic progression, cortical neuronal development, and neuronal migration. Despite their similarity and seemingly overlapping functions, further research showed their pathophysiological roles to be distinct. Additionally, NDE1 and NDEL1 undergo significant post-

translational modifications that are notably different and potentially facilitate a more refined level of regulation over their roles in the cell.

1.2.5.1. Role of NDE1 and NDEL1 in the dynein transport pathway

In eukaryotes, the microtubule cytoskeleton is formed from specific tubulin proteins that are assembled into polar microtubules. Cytoplasmic dynein-1 (dynein) and kinesins are proteins that act as molecular motors, regulating various forms of cytoskeletal dynamics (11,56). These proteins interact with cellular cargo, which can include membrane-bound vesicles, organelles, mRNAs, and proteins, and travel along microtubules to facilitate cargo movement. The motors function in opposite directions, dynein moves cargo towards the negative, while most kinesins move towards the positive end of the microtubules. In addition, the building and separation of mitotic spindles are facilitated by the two proteins, as well as promoting transition between mitotic phases by delivering mitotic-spindle checkpoint proteins to kinetochores.

Dynein exists as a large dimeric assembly of non-catalytic subunits that serve as regulators or attachment points to different cargo types (57). However, unlike kinesins, dynein function requires the interaction of several proteins outside the dynein protein family, including dynactin, LIS1, NDE1 and NDEL1. Some of these are crucial for molecular motor function, like dynactin and LIS1, as their depletion results in loss of dynein function.

The dynein heavy chain (DHC) contains the N-terminal tail and the C-terminal motor domain, which contains of six AAA (ATPases associated with cellular activities) modules assembled into a ring formation (58–60). Located between the fourth and fifth AAA module, a short coiled-coil stalk contains the microtubule binding domain (MTBD) on its C-terminal end (Figure 4A). Opposite the C-terminal stalk, the N-terminal third of DHC, known as the tail, is connected to the AAA ring. Each of the two N-terminal tails serve as a

scaffold for a dynein intermediate chain (DIC), and a dynein light intermediate chain (DLIC) that have extended N-termini binding to three light chains (DLC) named TcTex, LC8 and Roadblock (58,61,62).
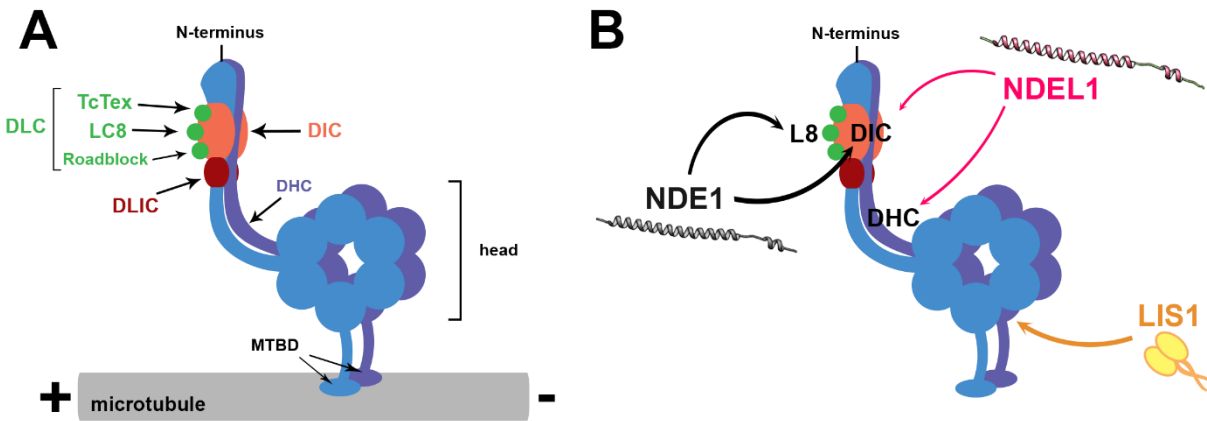
Figure 4. **Structure and interaction partners of cytoplasmic dynein 1.** (A) Simplified dynein dimeric structure with labelled chains. Heavy chains (DHC) are shown in blue, intermediate chains (DIC) in orange, light intermediate chains (DLIC) in burgundy and light chains (DLC) in green. The motor domain is contained in DHC and is shown as a ring formation of six circular AAA modules. Microtubule-binding domains (MTBD) are located at the C-terminal end of a coiled stalk-like structure. (B) LIS1 (yellow), NDE1 (black) and NDEL1 (pink) play roles in the dynein transport pathway. NDE1 and NDEL1 both interact with DIC with their N-terminal coiled coil domain. NDE1 can also bind to light chain 8 (LC8), while NDE1 binds to DHC. LIS1 binds between the third and fourth AAA module in the dynein motor domain, and the binding site is marked with the yellow arrow.

For its activity, dynein requires to be complexed with dynactin, a protein that enables dynein recruitment to the positive microtubule end, as well as cargo recognition and transport initiation (62). In addition, there are additional proteins containing coiled-coil structures that have been demonstrated to stimulate the motility of dynein-dynactin complexes. These coiled-coil proteins

are named activating adaptors, serving a dual function of not only enhancing motility of the complex, but also linking it to cargoes.

LIS1 is a functional dimer that is capable of binding between the third and fourth AAA module in dynein via its C-terminal β-propeller domain (Figure 4B) (63). Several studies have shown that by interacting with dynein, LIS1 modulates its binding affinity for microtubules if dynactin and an activating adaptor are not present (11). On the other hand, in their absence, LIS1 facilitates the activation of the dynein complex by inhibiting its inactive conformation.

Both NDE1 and NDEL1 can bind LIS1 and dynein, with slight differences in the region of dynein that they bind to (Figure 4B). NDE1 can bind the DIC with its N-terminal coiled-coil domain, and the LC8 with a short binding site found in the flexible linker region (11). In NDEL1, the N-terminal coiled-coil domain also contains a DIC binding site, and the predicted α-helical structure binds to DHC. Several *in vitro* studies showed evidence that NDE1 and NDEL1 are involved in increasing the affinity between LIS1 and dynein, acting as tethers. Interestingly, some *in vitro* studies on mammalian proteins showed evidence against the proposed tether model. Instead of increasing LIS1 binding affinity for dynein, NDE1 and NDEL1 decreased dynein's affinity to bind to microtubules (11,64). LIS1 has also been shown to promote binding between dynein and dynactin, while NDE1 and NDEL1 compete with dynactin (11,65).

Given the presence of contradictory findings, novel hypotheses regarding the role of NDE1 and NDEL1 within the dynein transport pathway have emerged (11). Due to their competitive binding with dynactin and ability to decrease dynein microtubule binding affinity, it is plausible that NDE1 and NDEL1 serve as scaffolds for LIS1 and dynein co-localization, simultaneously inhibiting the dynein-activating effect of LIS1. This state could persist until an unknown

trigger prompts LIS1-mediated dynein activation, its interaction with dynactin and activating adaptors, and release of NDE1 and NDEL1.

1.2.5.2. CENP-F-mediated function of NDE1 and NDEL1 in mitosis

Dynein plays multiple roles during mitosis. A fraction of dynein/dynactin complexes localizes to the kinetochore, a three-layered protein structure situated on chromosomes that is responsible for microtubule attachment and chromosome separation (66). When associated with the kinetochores, dynein propels the movement of chromosomes towards the cell poles and generates tension between sister kinetochores. The association has been shown to be mediated by the presence of NDE1 and NDEL1 at the kinetochores, as they appear at the site before dynein, dynactin or LIS1 (67).

Centrosome protein F (CENP-F), also known as mitosin, is a cell cycle regulated protein that exhibits a dynamic localization pattern (68). In early prophase, CENP-F accumulates at kinetochores, where it remains until the onset of late anaphase. In both NDE1 and NDEL1, binding sites for CENP-F have been identified in their C-terminal regions, and it has been shown that they are recruited to kinetochores by direct interaction (37,66). While CENP-F is responsible for their recruitment, studies have shown that its depletion does not completely abolish NDEL1 presence at kinetochores, suggesting there are multiple factors responsible for recruitment (66). Interestingly, NDE1 and NDEL1 are localized to kinetochores well before dynein, dynactin or LIS1. Studies have shown that NDEL1 depletion reduced dynein recruitment to kinetochores, as well as the inhibition of its stabilizing effect on kinetochore-bound dynein. Furthermore, interruption of NDEL1 function blocked mitotic progression before metaphase.

1.2.5.3. NDEL1-mediated neurofilament assembly

Neurofilaments are intermediate filaments that provide structural support in central nervous system neurons, particularly in the axons (69). They are

composed as heteropolymers of four distinct subunits, each containing diverse domain structures and functions: neurofilament light (NF-L), neurofilament middle (NF-M), neurofilament heavy (NF-H) and α-internexin or peripherin (70). NF-L, α-internexin, and peripherin exhibit the capacity to create 10-nanometer filaments, with NF-L primarily constituting the backbone. NF-M and NF-H are obligate heteropolymers and require the presence of NF-L for filaments to be formed.

In vivo studies characterized neurofilaments to have crucial roles in regulating neuron integrity and viability, specifically in axon transportation, nerve conduction and growth and upkeep of myelinated axons (34). Larger myelinated axons express NF-L and NF-H abundantly, contributing to the radial growth of axons (69). In regular circumstances, small amounts of NF-L are released from axons in an age-related manner, with higher amounts being released in individuals of older age. However, cases involving inflammation, neurodegeneration, trauma, or vascular damage can lead to axonal injuries, resulting in a significant increase in NF-L levels in cerebrospinal fluid in blood. Because of this, NF-L could potentially serve as a diagnostic tool for monitoring biomarkers in neurological diseases.

Nguyen et al. demonstrated that NDEL1 interacts with soluble NF-L subunits via its C-terminal region spanning residues 191-345 (Figure 3A) (34). Alongside its direct interaction with the NF-L rod domain, NDEL1 also establishes an indirect connection with NF-H. It's important to note that although NDEL1 interacts with these neurofilament subunits, it does not assemble with them. Instead, it plays a role in facilitating the assembly and homeostasis of the neurofilamentous network. When NDEL1 expression was reduced *in vitro*, neurofilament assembly was altered, and the assemblies contained cell organelles and Golgi apparatus fragments. Furthermore, abolishing NDEL1 expression in postnatal murine neurons showed similar

results, reminiscent of neurofilament assembly abnormalities associated with neurodegenerative disorders.

1.2.5.4. Phosphorylated NDEL1-mediated microtubule-severing activity of katanin

Katanin is a heterodimeric AAA protein complex composed of the catalytic ATPase containing A-subunit (KATNA1, also known as p60) and a regulatory B-subunit (KATNB1, also known as p80) (71). This microtubule-severing protein is localized to mitotic spindles and plays a crucial role in key cellular processes including cytoskeleton reorganization, cell division and migration, post-mitotic cell ciliation, and homeostasis (71,72).

Throughout interphase, microtubules vital for cell shape, transport and motility extend radially from the centrosome (71). Concentrating at centrosomes, KATNA1 and KATNB1 regulate the mitotic spindle's length, shape, and dynamics. As mitosis progresses, katanins are redistributed from the spindle to other microtubule-based structures. In telophase, KATNA1 is redistributed to the space between the central spindle bundle and the contractile ring. Importantly, this distribution occurs independently of the regulatory KATNB1 subunit. On the other hand, KATNB1 localizes differently during later mitotic stages, like anaphase, where it relocates to the spindle midzone. This variable redistribution highlights potential subunit-specific roles within mitosis.

Yeast two-hybrid studies showed that NDEL1 can bind the KATNA1 with its flexible linker region, and KATNB1 with its N-terminal coiled-coil domain (36). These studies also showed that LIS1 can also bind to katanin, but only to the regulatory KATNB1 subunit. Interestingly, introducing mutations in the Cdk5 or Cdc2 phosphorylation sites in the flexible linker region of NDEL1 greatly reduced its interaction KATNA1. Furthermore, while KATNA1 exhibited moderate affinity for unphosphorylated NDEL1, their binding affinity was

significantly enhanced by Cdk5 phosphorylation, which occurs at the centrosome during cell mitosis. By mediating katanin recruitment, NDEL1 might promote the formation of structures necessary for its function, initiating the reorganization of the microtubule network for chromosomal segregation and neuronal migration.

1.2.5.5. Endooligopeptidase NDEL1 activity

Endooligopeptidase A (EOPA) is an endopeptidase that has been found to correspond to the same protein as NDEL1 (73). Following this finding, the protein was no longer referred to as EPOA, but rather NUDEL-oligopeptidase, or more simply, just NDEL1. This cysteine protease is sensitive to thiol compounds that activate its enzymatic activity of cleaving several short peptides in the brain that are believed to influence learning, memory, and mood (17,74).

Some oligopeptidases exhibit specificity in recognizing cleavage sequence motifs, which is a characteristic not shared by NDEL1 (17). Its recognition sequence has yet to be determined, and cleavage substrate locations are therefore difficult to predict. Interestingly, DISC1 can competitively bind and therefore inhibit the protease activity of NDEL1 (75). This interaction also impacts processes such as neurite outgrowth and neuronal migration during embryogenesis, highlighting NDEL1's involvement in neurodevelopment.

1.2.5.6. NDE1 can prevent DNA damage in cell nuclei

Cohesin is a critical regulator of chromatin structures that exhibits several roles when complexed with its respective interaction partners (17,76,77). One of its essential functions is preserving the structural integrity of genomic regions and ensuring the cohesion of sister chromatids around centromeres. Previous research showed that NDE1 translocates translocate into cell nuclei, where it engages in interactions with cohesin and chromatin complexes related

to cohesion, indicating its protective role in DNA synthesis (S) heterochromatin remodelling.

In vitro studies showed that Ndel1 knockout in mice contributed to increased DNA damage, which was detected by specific immunosignals representing identifiers for DNA double strand breaks (76). This DNA damage highly contributed to an increase in DNA lesions within the developing cortex and ultimately disrupted normal cell cycle progression.

In summary, NDE1 co-regulates S phase progression and prevention of DNA damage. Intriguingly, this function has not been identified in NDEL1, which is primarily localized to the cell cytoplasm, while NDE1 is found to be highly expressed in cell nuclei and the perinuclear area of astrocytes (10).

1.2.5.7. NDE1 and NDEL1 exhibit distinctive functions

At first glance, NDE1 and NDEL1 seem to share several interaction partners, as well as functions, however, there are notable differences in their roles (Figure 5). In the dynein-mediated transport pathway they are thought to have identical roles, but because of their different binding sites on dynein, it is likely their function is not completely synonymous. Furthermore, the current understanding of the dynein-mediated transport system is largely unknown and is based on hypothesised models. Another shared function is mediated by CENP-F, which recruits NDE1 and NDEL1 to kinetochores during mitosis.

Other known protein functions differ between the paralogs and may be caused by differences in NDE1 versus NDEL1 expression and regulation. NDEL1 can bind neurofilaments to facilitate the assembly of the neurofilamentous network. Additionally, it mediates katanin recruitment, and therefore promotes microtubule network organization that is crucial for chromosomal segregation and neuronal migration. Previously known as EOPA, NDEL1 exhibits oligopeptidase activity and cleaves short peptides found in the brain. Remarkably, these functions are exclusively associated with NDEL1, with no

indication of their presence in NDE1. However, NDE1 displays its own distinctive function by entering cell nuclei, where it plays a role in preventing DNA damage, a functional role that has not been found in NDEL1.
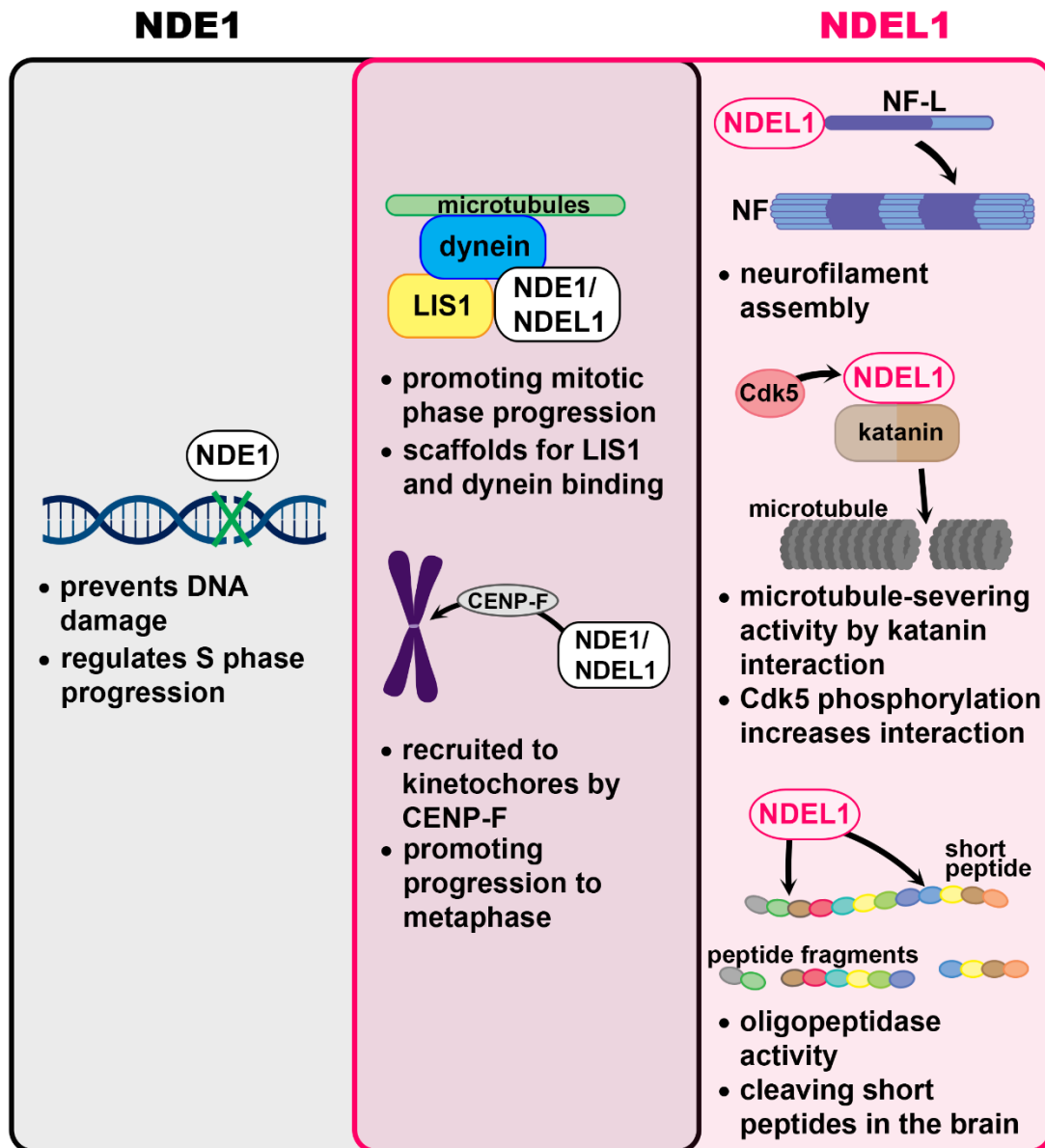

Figure 5. **NDE1 and NDEL1 proteins differ in their cellular functions.** The left (grey) column summarizes functions found only in NDE1, and the right (pink) column summarizes NDEL1-specific functions. The middle, overlapping column shows functions that seem to be present in both proteins, and can be considered the main roles of the paralogs.

1.3. Rare versus common codon usage

The genetic code allows the existence 64 different trinucleotide codons, three of which code for terminating translation. Other codons are used to encode the 20 standard amino acids, 18 of which are encoded by two to six synonymous codons (Figure 6A) (78,79). Historically, these synonymous codons were considered interchangeable since they don't modify the protein's amino acid sequence, and mutations preserving the amino acid were labelled as silent. However, evidence emerged that within genomes there is codon usage bias, the preferential usage of certain synonymous codons (80). As synonymous codons exhibit varying frequency in being recognized by cognate tRNAs, codon usage bias correlates with tRNA quantities in different organisms (Figure 6B). Codon prevalence across organisms can also be influenced by the proportion of GC-base pairs present.

A

Second base position

First base position	U		C		A		G		Third base position
U	UUU	¹P	UCU	S	UAU	Y	UGU	C	U
	UUC		UCC		UAC		UGC		C
	UUA	L	UCA		UAA	Stop	UGA	Stop	A
	UUG		UCG		UAG		UGG	W	G
C	CUU	L	CCU	P	CAU	H	CGU	R	U
	CUC		CCC		CAC		CGC		C
	CUA		CCA		CAA	Q	CGA		A
	CUG		CCG		CAG		CGG		G
A	AUU	I	ACU	T	AAU	N	AGU	S	U
	AUC		ACC		AAC		AGC		C
	AUA		ACA		AAA	K	AGA	R	A
	AUG	M	ACG		AAG		AGG		G
G	GUU	V	GCU	A	GAU	D	GGU	G	U
	GUC		GCC		GAC		GGC		C
	GUA		GCA		GAA	E	GGA		A
	GUG		GCG		GAG		GGG		G

¹The one letter symbol of amino acids.

B

Codon triplet	Frequency (per thousand)	Codon triplet	Frequency (per thousand)	Codon triplet	Frequency (per thousand)	Codon triplet	Frequency (per thousand)
UUU	17.6	UCU	15.2	UAU	12.2	UGU	10.6
UUC	20.3	UCC	17.7	UAC	15.3	UGC	12.6
UUA	7.7	UCA	12.2	UAA	1.0	UGA	1.6
UUG	12.9	UCG	4.4	UAG	0.8	UGG	13.2
CUU	13.2	CCU	17.5	CAU	10.9	CGU	4.5
CUC	19.6	CCC	19.8	CAC	15.1	CGC	10.4
CUA	7.2	CCA	16.9	CAA	12.3	CGA	6.2
CUG	39.6	CCG	6.9	CAG	34.2	CGG	11.4
AUU	16.0	ACU	13.1	AAU	17.0	AGU	12.1
AUC	20.8	ACC	18.9	AAC	19.1	AGC	19.5
AUA	7.5	ACA	15.1	AAA	24.4	AGA	12.2
AUG	22.0	ACG	6.1	AAG	31.9	AGG	12.0
GUU	11.0	GCU	18.4	GAU	21.8	GGU	10.8
GUC	14.5	GCC	27.7	GAC	25.1	GGC	22.2
GUA	7.1	GCA	15.8	GAA	29.0	GGA	16.5
GUG	28.1	GCG	7.4	GAG	39.6	GGG	16.5

Figure 6. **Synonymous codons encode for the 20 standard amino acids.** (A) The universal genetic code chart adopted from Sanchez et al. (81). (B) Codon frequency values in humans. Data obtained from the Codon Usage Database (http://www.kazusa.or.jp/codon/) (82).

Common codons show higher prevalence in an organism and are found as enriched in genes encoding for highly expressed proteins (79,80). The preference for common codon usage can be attributed to faster translation and enhanced protein sequence accuracy. Conversely, more infrequent codons, known as rare codons, are thought to be responsible for slower translation speed, modulating translational protein folding, and lower protein expression (80).

Despite being very similar in structure, there are functional differences between NDE1 and NDEL1. These differences could be due to subtle variations in their amino acid sequences (Figure 2), which might influence their interactions with other proteins or cellular processes. Interestingly, their nucleic acid sequences are surprisingly divergent, with *NDE1* containing a higher proportion of GC-base pairs compared to *NDEL1* (55.1% and 45.6% respectively). The variations in nucleic acid sequence in human *NDE1* and *NDEL1* genes seem to influence the frequency of common versus rare codon usage between the proteins. This represents an area of difference between the proteins that remains unexplored. However, it could influence protein expression levels, protein folding, or even the localization of these proteins within cells.

1.3.1. Designing codon switched plasmids

Codon recoding is a process involving replacing codons with a synonymous alternative in a way that is mRNA-specific but does not impact the genetic code (83,84). However, to investigate whether rare codon bias in *NDE1* and *NDEL1* sequences affects their expression levels, it was necessary to study plasmids containing genes for switched codon proteins. Specifically, the plasmids were to encode for NDE1 proteins with NDEL1-like codons (NDE1-NLc) and NDEL1 with NDE1-like codons (NDEL1-Nc).

Figure 7. **Nucleic base sequence alignment of wild type and switched codon NDE1 and NDEL1 constructs**. Conserved residues are highlighted in red, while residues that were conservatively substituted are highlighted in yellow. Sequences were aligned using the MUSCLE algorithm in MEGA software (85), and the figure was generated with ESPript v3.0 (www.espript.ibcp.fr) (27).

```
              1         10        20        30        40        50
NDE1_WT    .MEDSGKTFSSEEEEANYWKDLAMTYKQRAENTQEELREFQEGSREYEAELETQLQQIET
NDE1_NLc   .MEDSGKTFSSEEEEANYWKDLAMTYKQRAENTQEELREFQEGSREYEAELETQLQQIET
NDEL1_WT   MDGEDIPDFSSLKEETAYWKELSLKYKQSFQEARDELVEFQEGSRELEAELEAQLVQAEQ
NDEL1_Nc   MDGEDIPDFSSLKEETAYWKELSLKYKQSFQEARDELVEFQEGSRELEAELEAQLVQAEQ

              60        70        80        90        100       110
NDE1_WT    RNRDLLSENNRLRMELETIKEKFEVQHSEGYRQISALEDDIAQTKAIKDQLQKYIRELEQ
NDE1_NLc   RNRDLLSENNRLRMELETIKEKFEVQHSEGYRQISALEDDIAQTKAIKDQLQKYIRELEQ
NDEL1_WT   RNRDLQADNQRLKYEVEALKEKLEHQYAQSYKQVSVLEDDLSQTRAIKEQLHKYVRELEQ
NDEL1_Nc   RNRDLQADNQRLKYEVEALKEKLEHQYAQSYKQVSVLEDDLSQTRAIKEQLHKYVRELEQ

              120       130       140       150       160       170
NDE1_WT    ANDDLERAKRATIMSLEDFEQRLNQAIERNAFLESELDEKENLLESVQRLKDEARDLRQE
NDE1_NLc   ANDDLERAKRATIMSLEDFEQRLNQAIERNAFLESELDEKENLLESVQRLKDEARDLRQE
NDEL1_WT   ANDDLERAKRATIVSLEDFEQRLNQAIERNAFLESELDEKESLLVSVQRLKDEARDLRQE
NDEL1_Nc   ANDDLERAKRATIVSLEDFEQRLNQAIERNAFLESELDEKESLLVSVQRLKDEARDLRQE

              180       190       200       210       220       230
NDE1_WT    LAVQQKQE...KPRTPMPSSVEAERTDTAVQATGSVPSTPIAHRGPSSSLNTPGSFRRGL
NDE1_NLc   LAVQQKQE...KPRTPMPSSVEAERTDTAVQATGSVPSTPIAHRGPSSSLNTPGSFRRGL
NDEL1_WT   LAVRERQQEVTRKSAPSSPTLDCEKMDSAVQASLSLPATPVG.KGTENTFPSPKAIPNGF
NDEL1_Nc   LAVRERQQEVTRKSAPSSPTLDCEKMDSAVQASLSLPATPVG.KGTENTFPSPKAIPNGF

              240       250       260       270       280       290
NDE1_WT    DDSTGGTPLTPAARISALNIVGDLLRKVGALESKLASCRNLVYDQSPNR...TGGPASGR
NDE1_NLc   DDSTGGTPLTPAARISALNIVGDLLRKVGALESKLASCRNLVYDQSPNR...TGGPASGR
NDEL1_WT   ....GTSPLTPSARISALNIVGDLLRKVGALESKLAACRNFAKDQASRKSYISGNVNCGV
NDEL1_Nc   ....GTSPLTPSARISALNIVGDLLRKVGALESKLAACRNFAKDQASRKSYISGNVNCGV

              300       310       320       330
NDE1_WT    SSKNRDGGERRPSSTSVPLGD.KGLDTSCRWLSKSTTRSSSSC.......
NDE1_NLc   SSKNRDGGERRPSSTSVPLGD.KGLDTSCRWLSKSTTRSSSSC.......
NDEL1_WT   LNGNGTKFSRSGHTSFFDKGAVNGFDPAPPPPGLGSSRPSSAPGMLPLSV
NDEL1_Nc   LNGNGTKFSRSGHTSFFDKGAVNGFDPAPPPPGLGSSRPSSAPGMLPLSV
```
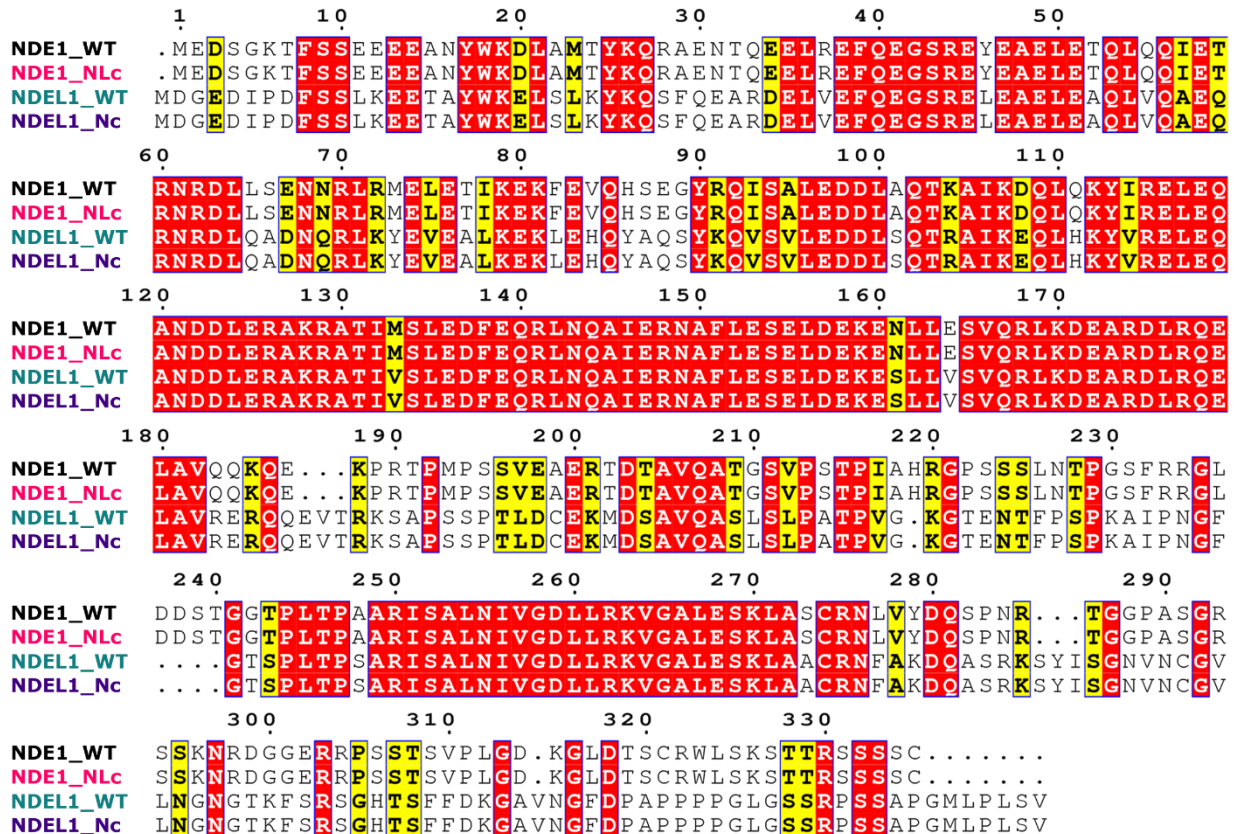
Figure 8. **Amino acid sequence alignment of wild type and switched codon NDE1 and NDEL1 constructs**. Conserved residues are highlighted in red, while residues that were conservatively substituted are highlighted in yellow. Sequences were aligned using the MUSCLE algorithm in MEGA software (85), and the figure was generated with ESPript v3.0 (www.espript.ibcp.fr) (27).

The switched codon genetic sequences were designed by aligning human NDE1 and NDEL1, allowing a systematic comparison of each codon within the sequences (Bradshaw, unpublished). When the same amino acid was present in both proteins, the corresponding codon from the gene being "mimicked" was used in place of the original wild type codon. In cases where a different amino acid was present at a specific position, all synonymous codons were

examined, and the one with a rarity closest to the gene being "mimicked" was chosen. If an amino acid existed in the wild type gene but no amino acid existed in the same portion of the gene being "mimicked", a codon was selected based on its similarity in rarity to the codons immediately adjacent to it. These newly designed NDE1-NLc and NDEL-Nc sequences were then synthesised commercially. Alignment of both nucleic acid (Figure 7) and amino acid (Figure 8) sequences of wild type and switched codon sequences demonstrates that, while sequences vary in nucleic acids, they are identical amino acid residues.

2. Aim of the thesis

NDE1 and NDEL1 share highly similar protein structures and over 50% of amino acid sequence similarity, but show differences in their nucleic acid sequences, expression levels and functions in cellular processes. In addition, these paralogs are associated with some neurological disorders, including schizophrenia and lissencephaly, and may potentially play key roles in their development. Rare codon usage frequency remains an unexplored area of research when it comes to human *NDE1* and *NDEL1* genes, as NDEL1 seems to show a higher frequency of rare codons. We hypothesize that differences in rare codon bias between NDE1 and NDEL1 lead to alterations in their expression, which may contribute to functional differences.

In this thesis we aimed to:

1) Determine differences in rare codon usage in human *NDE1* and *NDEL1* genes.
2) Investigate if the differences in rare codon usage seen in the human *NDE1* and *NDEL1* genes are also conserved across other vertebrate genera.
3) Determine whether there are differences in the expression of wild type and switched codon NDE1 and NDEL1 in HEK293 cells transfected with FLAG-tagged proteins.
4) Confirm results from the previous aim using an alternative expression system, specifically in HEK293 cells transfected with V5-tagged proteins.
5) Compare the expression patterns of wild type and switched codon NDE1 and NDEL1 in HEK293 cells using fluorescent microscopy.

3. Materials and methods

3.1. Materials

3.1.1. DNA Plasmids

Table 1. List of used DNA plasmids. All plasmids were unpublished and generated by Nicholas J. Bradshaw at the Heinrich Heine University, Düsseldorf. Wild type proteins are labelled with WT. Nc and NLc label the codon set used to encode for the protein due to differences in rare codon bias between the proteins. NDE1-NLc are NDE1 proteins encoded by codons that match those in NDEL1-WT, while maintaining the appropriate amino acid sequence. NDEL1-Nc are NDEL1 proteins encoded by NDE1-WT codons.

Vector	Protein encoded	Antibiotic resistance
pdcDNA-FlagMyc	NDE1-WT	Ampicillin
pdcDNA-FlagMyc	NDEL1-WT	Ampicillin
pdcDNA-FlagMyc	NDE1-NLc	Ampicillin
pdcDNA-FlagMyc	NDEL1-Nc	Ampicillin
pMAX	NDE1-WT	Kanamycin
pMAX	NDEL1-WT	Kanamycin
pMAX	NDE1-NLc	Kanamycin
pMAX	NDEL1-Nc	Kanamycin

3.1.2. Commercially available kits, stains, and size markers

Table 2. List of used commercially available kits and stains.

Name	Supplier
my-Budget DNA/RNA Stain Green	Bio-Budget Technologies GmbH
10x FastDigest Green Buffer	Thermo Fisher Scientific
Pierce ECL Western Blotting Substrate	Thermo Fisher Scientific
QIAprep Spin Miniprep Kit	QIAGEN

Table 3. List of used size markers.

Name	Description	Supplier
my-Budget 1 kb DNA ladder (200 µg/mL)	Suitable for sizing double-stranded DNA in the range between 250 base pairs and 10 kilobase pairs.	Bio-Budget Technologies GmbH
my-Budget Prestained Protein Ladder 10-180 kDa (0.2-0.4 µg/µL)	Suitable for sizing proteins in the size ranges between 10 kDa and 180 kDa.	Bio-Budget Technologies GmbH

3.1.3. Antibodies

Table 4. List of primary antibodies used in Western blot and immunocytochemistry.

Name	Supplier	Host	Concentration	Dilution
Anti-FLAG M2	Sigma	mouse	1 mg/mL	1:2000 for Western blotting, 1:1000 for immunocytochemistry.
V5 tag	Thermo Fisher Scientific	mouse	1 mg/mL	1:2000
Anti-β-actin	Sigma	mouse	1 mg/mL	1:10000

Table 5. List of secondary antibodies used in Western blot.

Name	Supplier	Concentration	Dilution
Horseradish peroxidase conjugated affinity purified goat anti-mouse IgG	Thermo Fisher Scientific	1 mg/mL	1:10000 for samples stained with anti-FLAG M2 or V5 tag primary antibodies. 1:5000 for samples stained with anti-β-actin primary antibody.

Table 6. List of secondary antibodies and stains used in immunocytochemistry.

Name	Supplier	Concentration	Dilution
Alexa Fluor 555 Goat anti-Mouse IgG	Thermo Fisher Scientific	2 mg/mL	1:10000
Phalloidin-iFlour 488 Reagent	Abcam	1000x stock solutions	1:500
DAPI	Sigma	1 mg/mL	1:500

3.1.4. Gels

Agarose gel (handmade)

Table 7. Measurements and materials for a handmade agarose gel. 50x TAE stock solution was prepared using 242 g Tris, 18.61 g EDTA, 57.1 mL acetic acid and adding dH$_2$O up to 1 L.

Agarose	0.5 g
1x TAE buffer	50 mL
DNA stain	1 µL

10% Acrylamide running gel (handmade)

Table 8. Measurements and materials for a 10% handmade acrylamide running gel. 30% acrylamide was prepared using 14.6 g acrylamide, 0.5 g N,N'-methylbisacrylamide and adding dH_2O up to 100 mL.

dH₂O	4.8 mL
30% acrylamide	3.9 mL
1.5 M Tris [pH 8.8]	3 mL
10% SDS	120 μL
10% APS	120 μL
TEMED	12 μL

Acrylamide stacking gel (handmade)

Table 9. Measurements and materials for a handmade acrylamide stacking gel. 30% acrylamide was prepared using 14.6 g acrylamide, 0.5 g N,N'-methylbisacrylamide and adding dH_2O up to 100 mL.

dH₂O	2.6 mL
30% acrylamide	1 mL
1 M Tris [pH 6.8]	625 μL
10% SDS	50 μL
10% APS	50 μL
TEMED	5 μL

Casting of both acrylamide gels was performed using the Mini-PROTEAN Tetra Handcast Systems (Bio-Rad). After assembling the gel holders, running gel components were well mixed in a 50 mL Falcon tube, and the gel was poured between the two glass plates, leaving 1 centimetre empty towards the top of the glass. The empty volume was temporarily filled with dH_2O until the gel

solidified. Afterwards, the water was poured off, and the stacking gel mixture was poured in the empty volume above the running gel, and well combs were added before letting the gels to completely set on room temperature.

3.2. Methods

3.2.1. Rare codon analysis

Protein coding nucleotide sequences of NDE1 and NDEL1 for several species (Table 10) were obtained using the UCSC Genome Browser (www.genome-euro.ucsc.edu) (23). The rare codon usage was analysed using the Clark Lab Rare Codon Calculator (www.codons.org) (79). The Rare Codon Calculator gives %MinMax values as output, which indicates whether the given gene sequences use common or rare codons. Codon usage data for each organism was obtained using the Codon Usage Database (http://www.kazusa.or.jp/codon/) (82). Rare codon usage frequency was compared across individual species and groups to determine evolutionary conservation.

Table 10. Accession numbers of analysed mRNA sequences of NDE1 and NDEL1 across multiple species. Acession numbers beginning with the prefix NM correspond to curated records, while those with the prefix XM are model records that have not been reviewed.

Group	Species		NDE1 accession number	NDEL1 accession number
human	human	*Homo sapiens*	NM_017668	NM_030808
non-human primates	chimpanzee	*Pan troglodytes*	XM_016929502.1	NM_001280356.1
	western lowland gorilla	*Gorilla gorilla gorilla*	XM_019011958.2	XM_004058561.2
	Sumatran orangutan	*Pongo abelii*	XM_009250496.2	NM_001132583.1

	Bolivian squirrel monkey	*Saimiri boliviensis boliviensis*	XM_010332603.1	XM_003929225.2
	olive baboon	*Papio anubis*	XM_009196068.3	XM_021928729.1
	mouse lemur	*Microcebus murinus*	XM_012790229.1	XM_012775242.1
non-primate mammals	house mouse	*Mus musculus*	NM_023317	NM_023668
	Norway rat	*Rattus norvegicus*	NM_053347.2	NM_133320.2
	rabbit	*Oryctolagus cuniculus*	XM_002711777.3	NM_001082020.1
	pig	*Sus scrofa*	XM_021086166.1	NM_001243862.1
	horse	*Equus caballus*	XM_023616274.1	XM_023653473.1
	dog	*Canis lupus familiaris*	NM_001252172.1	XM_038516145.1
non-mammalian vertebrates	chicken	*Gallus gallus*	NM_001006169.1	NM_001030696.1
	Zebra finch	*Taeniopygia guttata*	XM_002197893.3	XM_012578526.1
	American alligator	*Alligator mississippiensis*	XM_006261583.1	XM_006277040.1
	Common garter snake	*Thamnophis sirtalis*	XM_014070034.1	XM_014055954.1
	African clawed frog	*Xenopus laevis*	NM_001088345.1	NM_001092863.1
	Western clawed frog	*Xenopus tropicalis*	NM_001007995.1	NM_001016201.2

3.2.2. Growth of plasmids in bacterial culture

Plasmids encoding NDE1 or NDEL1 proteins were transformed into competent NEB5α (New England Biolabs) bacteria, an *E. coli* strain. For each transformation, 1 µL of plasmid DNA was added to 50 µL freshly thawed

bacteria in a 1.5 mL Eppendorf tube and incubated on ice for 30 minutes. The bacterial suspension was heat-shocked at 42 $^{\circ}$C for 30 seconds and afterwards placed on ice for 5 minutes to allow bacteria to recover. For plasmids in pMAX vectors that were resistant to kanamycin, 250 µL of fresh LB Media (1 g tryptone, 0.5 g yeast extract, 0.5 g NaCl, dH$_2$O up to 100 mL, sterilised by autoclaving) was added to the Eppendorf tubes which were left to incubate in a shaking incubator for 45 minutes at 37 $^{\circ}$C and 250 rpm. Whole volumes in Eppendorf tubes were spread onto LB agar (1 g tryptone, 0.5 g yeast extract, 0.5 g NaCl, 1.5 g agar, dH$_2$O up to 100 mL, sterilised by autoclaving) plates containing appropriate antibiotics, and bacteria were grown overnight in an incubator at 37 $^{\circ}$C and 5% CO$_2$.

Liquid bacterial cultures were set up following the overnight incubation of transformed bacteria on LB agar plates. 3 mL of LB media was added into a 15 mL Falcon tube, followed by the addition of the appropriate antibiotic (100 µL/mL). A single bacterial colony was picked and added into the Falcon tube, after which the cultures were left in the shaking incubator overnight at 37 $^{\circ}$C and 250 rpm.

3.2.3. Plasmid DNA purification from bacteria

To purify plasmid DNA, liquid bacterial cultures were centrifuged for 10 minutes at 3700 rpm, the supernatant was discarded, and the pellet was kept. Using the Qiagen QIAprep Spin Miniprep Kit and the appropriate manufacturer's protocol, plasmid DNA was eluted from the bacterial pellet. Briefly, the pellet was resuspended in 250 µL P1 buffer and transferred to a clean 1.5 Eppendorf tube. Cells were lysed by adding 250 µL P2 buffer and incubated at room temperature for 2 minutes. Lysis was terminated by addition of 350 µL N3 buffer and samples were centrifuged for 10 minutes at 13000 rpm. The supernatant was transferred to QIAprep 2.0 columns and centrifuged for 1 minute at 13000 rpm, discarding the flow-through. Columns were washed with 750 µL PE buffer and centrifuged twice for 1 minute at

13000 rpm, discarding the flow-through both times. Plasmid DNA was eluted from the column using 50 µL EB buffer (10 mM Tris-Cl [pH 8.5]), leaving the buffer on the column for 1 minute at room temperature before eluting by centrifugation for 1 minute at 13000 rpm.

Following plasmid purification, sample concentration was measured using a BioDrop µLITE spectrophotometer with the absorbance wavelength set to 260 nm. Baseline concentration was measured using EB buffer as a blank, and sample concentrations were expressed in µL/mL.

3.2.4. Agarose gel electrophoresis

Purified DNA length was determined by agarose gel electrophoresis, separating plasmid DNA by their size. Agarose gel was made by heating the mixture of 0.5 g agarose and 50 mL 1x TAE buffer (50x stock solution; 242 g Tris, 18.61 g EDTA, 57.1 mL acetic acid, dH_2O added up to 1 L) until the components fully combined. The gel was left to cool down until the beaker containing the mixture could be comfortably touched by hand. 1 µL DNA stain was added and the gel was poured into a preassembled holder with well combs in place, leaving it at room temperature to set. When ready, the gel was transferred into an electrophoresis dish filled with 1x TAE buffer. Samples were prepared by adding 7 µL dH_2O, 2 µL plasmid DNA and 1 µL Green buffer into a 1.5 mL Eppendorf tube. DNA marker was prepared by combining 2.5 µL DNA ladder and 0.5 µL Green buffer. Whole volumes of samples and the DNA marker prepared in the Eppendorf tubes were loaded into appropriate wells, and electrophoresis was run for 15 minutes at 140 V. Gel images were obtained using the Bio-Rad ChemiDoc Imaging System.

3.2.5. Plasmid DNA sequencing

Sequencing results were obtained using Eurofins Genomics Europe Sequencing GmbH services. Before sending out, samples were prepared by adding 2.5 µL of the appropriate primer to a 1.5 mL Eppendorf tube. Plasmid

DNA volume was determined by its concentration, aiming for 400 to 500 ng of plasmid in the sequencing sample. The total volume of 10 μL in the Eppendorf tube was reached by adding dH_2O.

3.2.6. Mammalian cell culture and transfection

HEK293 human embryonic kidney cell line was grown in T25 flasks or 12-well plates containing DMEM media (Thermo Fisher Scientific) with 10% foetal calf serum, 1x penicillin and streptomycin solution, and 1x MEM non-essential amino acids, referred to as DMEM +/+ media. Flasks and plates were kept in the incubator at 37 ^{o}C and 5% CO_2.When cells reached 80% confluency, they were split using Trypsine-EDTA.

Transfection was performed on HEK293 cells grown in 12-well plates using the reagent Metafectene (Biontex). During the transfection protocol, DMEM media with no added serum or antibiotics is used and is referred to as DMEM -/- media. Two sets of solutions were prepared in sterile 1.5 mL Eppendorf tubes: the first set containing 500 ng plasmid DNA and 100 μL DMEM -/- media, and the second 2 μL Metafectene and 100 μL DMEM -/- media. Both sets were left to incubate at room temperature for 5 minutes, after which the respective pairs from both sets were combined and incubated at 37 ^{o}C for 30 minutes. In the meantime, DMEM +/+ media in which the cells were grown was removed and any remnants were washed with DMEM -/- media once. 300 μL of DMEM -/- media was added to each well containing cells, followed by 200 μL of the plasmid DNA and Metafectene solution. The plates were incubated for 6 hours at 37°C and 5% CO_2, after which the media was removed and replaced with fresh DMEM containing serum and antibiotics. Transfected HEK293 cells were left in the incubator at 37°C and 5% CO_2 overnight, and afterwards lysed for Western blotting.

HEK293 cells that were used for immunocytochemistry and fluorescent microscopy required cells to be grown on glass coverslips before performing

the transfection. The protocol for transfecting was the same as with cells that were subsequently lysed for Western blotting, except Metafectene Pro (Biontex) being used as the transfecting reagent.

3.2.7. Mammalian cell lysis

The day after transfection HEK293 cells were lysed to use in Western blotting. Cell lysis buffer (5 mL 10x PBS, 5 mL 10% Trioton X-100, 1 mL 1M MgCl2, dH$_2$O added up to 50 mL) was prepared in advance and completed with DNase I (1 µL per 1 mL of buffer) and 1x protease inhibitor cocktail. Each well containing cells was washed twice with 500 µL 1x Phosphate buffered saline (PBS) (10x stock solution; 80 g NaCl, 2 g KCl, 14.4 g Na$_2$HPO$_4$, 2.4 g KH$_2$PO$_4$, MiliQ added up to 1 L, adjusted pH to 7.4), keeping the plates on ice. After the second wash, 100 µL lysis buffer was added and the plates were incubated for 5 minutes before transferring lysed cell suspension to clean and labelled 1.5 mL Eppendorf tubes. The tubes were incubated on the rotor for 30 minutes at room temperature. Following the incubation, 100 µL protein loading buffer (6.25 mL 1M Tris [pH 6.8], 10 mL glycerol, 20 mL 10% SDS, 3.75 mL dH$_2$O, approximately 5 mg of bromophenol blue) and 20 µL 1M dithiothreitol (DTT) was added to each tube, and samples were heated at 95 ^{o}C for 5 minutes to denature the proteins. The tubes were then placed on ice and could be used immediately in Western blots or stored at -20 ^{o}C.

3.2.8. SDS-PAGE and Western blot

To assemble SDS-PAGE equipment, handmade acrylamide running and stacking gels were prepared in the appropriate gel holder, which was placed into the appropriate dish. The space between two gels and the SDS-PAGE tank were filled with 1x Running buffer (10x stock solution; 30 g Tris, 144 g glycine, 10 g SDS, dH$_2$O added up to 1 L) up to the appropriate marks. Cell lysates and protein marker were loaded into wells in volumes of 15 µL and 2 µL, respectively. SDS-PAGE was run for 45 minutes at 180 V, when the dye front reached the bottom of the gels.

For transferring protein bands to a membrane, SDS-PAGE gels were removed from the holders and washed once with 1x Semi-dry transfer buffer (10x stock solution; 5.8 g Tris, 2.9 g glycine, 200 mL methanol, MiliQ added up to 1 L), and then incubated in fresh 1x Semi-dry transfer buffer for 10 minutes at room temperature on the shaker. Using the Transblot Turbo System (Bio-Rad) set to run for 30 minutes at 25V and 0.5 A for one gel or 1 A for two gels, protein bands were transferred a Parablot PVDF Membrane (Macherey-Nagel, 0.2 µm pore). To visualize total protein, membranes were stained with Ponceau S solution (1 g Ponceau S, 4 mL acetic acid, dH_2O added up to 200 mL).

After completing the transfer, membranes were incubated in PBS-Tween (100 mL 10x PBS, 500 µL Tween-20, MiliQ added up to 1) with 5% dry milk solution for an hour at room temperature on the shaker to block non-specific antibody binding. Remaining milk solution was washed with fresh PBS-Tween, and proteins of interest were detected by incubating membranes in the appropriate primary antibody diluted in PBS-Tween (Table 4) for 4 hours at room temperature on the shaker, or overnight at 4 °C. Primary antibody solutions contained 0.2% sodium azide and could be reused when stored at -20 °C. Secondary antibodies were diluted in PBS-Tween (Table 5), and membranes were incubated for one hour on the shaker. Following each incubation, membranes were washed three times in PBS-Tween for 10 minutes at room temperature on the shaker. Protein bands were visualized using the ECL Prime Western Blotting Substrate (Thermo Fisher Scientific) and Bio-Rad ChemiDoc Imaging System.

3.2.9. Protein level quantification following Western blotting

Protein expression levels were quantified using the Bio-Rad Image Lab software after membrane visualization and imaging. By manually adjusting the band lanes, the software provided complete reports on band identities, expressed as adjusted volumes determined via the integrated normalization

process. Adjusted volume values were obtained for FLAG-tagged and V5-tagged proteins, and the respective β-actin bands for each sample. β-actin bands were utilized to normalize samples for cell count variability. The obtained normalized volumes were averaged across technical replicates, and subsequently, data from all biological replicates were subjected to analysis using a two-way paired t-test and one-way ANOVA.

3.2.10. Western blot membrane stripping for re-staining

Removing antibodies bound to membranes following previous antibody staining was achieved by membrane stripping. Membranes were incubated in Mild Stripping Buffer (1.5 g glycine, 0.1 g SDS, 1 mL Tween-20, MiliQ added up to 100 mL, adjusted pH to 2.2) for 45 minutes at room temperature on the shaker, replacing the buffer three times, every 15 minutes. Afterwards, membranes were washed three times with PBS-Tween for 10 minutes on the shaker and were then ready to be blocked with the PBS-Tween and 5% milk solution. Stripping allowed the use of a different primary antibody to detect new proteins of interest.

3.2.11. Immunocytochemistry and microscopy

Transfected HEK293 cells grown on glass coverslips were washed once with 0.5 mL 1x PBS, fixed with 0.5 mL Fixation buffer (8 g paraformaldehyde, 20 mL 10x PBS, dH$_2$O added up to 200 mL, adjusted pH to 7.4) for 15 minutes and permeabolized with 0.5 mL Permeabolization buffer (10 mL 10% Triton X-100, 10 mL 10x PBS, dH$_2$O added up to 100 mL). Cells were washed briefly three times with 1 mL 1x PBS.

To block non-specific antibody binding, coverslips with transfected cells were incubated in 10% goat serum in 1x PBS for 45 minutes on the shaker at room temperature. After removing the blocking solution, cells were washed once briefly in 1x PBS and then incubated in the appropriate primary antibody (Table 4) diluted 1000-fold in 10% goat serum in 1x PBS for 3 hours on the

shaker at room temperature. Coverslips were washed three times with 1x PBS over a period of 15 minutes and then incubated in the secondary antibody, cytoskeletal and nuclear stain (Table 6), diluted in 10% goat serum in 1x PBS for 1 hour on the shaker in the dark. Following the incubation, three more washes with 1x PBS over a period of 15 minutes were performed, and coverslips were attached on microscopy slides with a commercial Mounting Medium Fluoroshield (Sigma).

Transfected HEK293 cells were viewed on an Olympus IX83 fluorescent microscope under 60x magnification. Images were taken by Hamamatsu Orca R2 CCD camera and CellSens software.

4. Results

4.1. Increased rare codon usage in *NDEL1* compared to *NDE1* is evolutionary conserved in mammalian species

As frequencies of synonymous codons often differ in a genome, they can be classified into rare or common ones (78). To investigate the frequency of rare codon usage in human *NDE1* and *NDEL1* genes, we used the Clark Lab Rare Codon Calculator program (www.codons.org) (79). This program quantifies codon rarity in a specific species as a figure %MinMax, in which positive %MinMax values represent widely used codons and negative values represent rarely used codons. Human *NDE1* sequence showed higher %MinMax values than *NDEL1* across most of the sequence length (Figure 9A). Average calculation values were compared by paired t-test that showed *NDEL1* having significantly lower values, suggesting an increased rare codon usage compared to *NDE1* (Figure 9B). Because increased rare codon frequencies have been associated with slower translation speed (80), this confirms that NDEL1 should be slower to translate than NDE1.
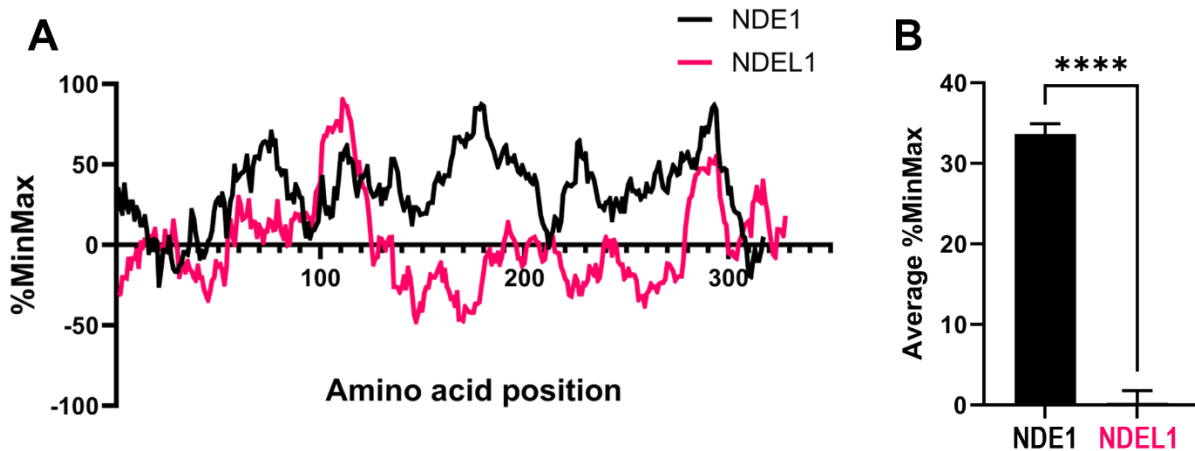
Figure 9. **Pairwise comparison of NDE1 and NDEL1 rare codon usage in humans.** (A) %MinMax value representing codon rarity for each amino acid position in *NDE1* and *NDEL1*, shown from N-terminus to C-terminus. (B) Average %MinMax value for *NDE1* and *NDEL1* codon usage, error bars show SEM. Rare codon usage was

calculated using the Clark Lab Rare Codon Calculator (www.codons.org) (79). Statistical analysis was performed by paired two-tailed t-test (****p ≤ 0.0001).
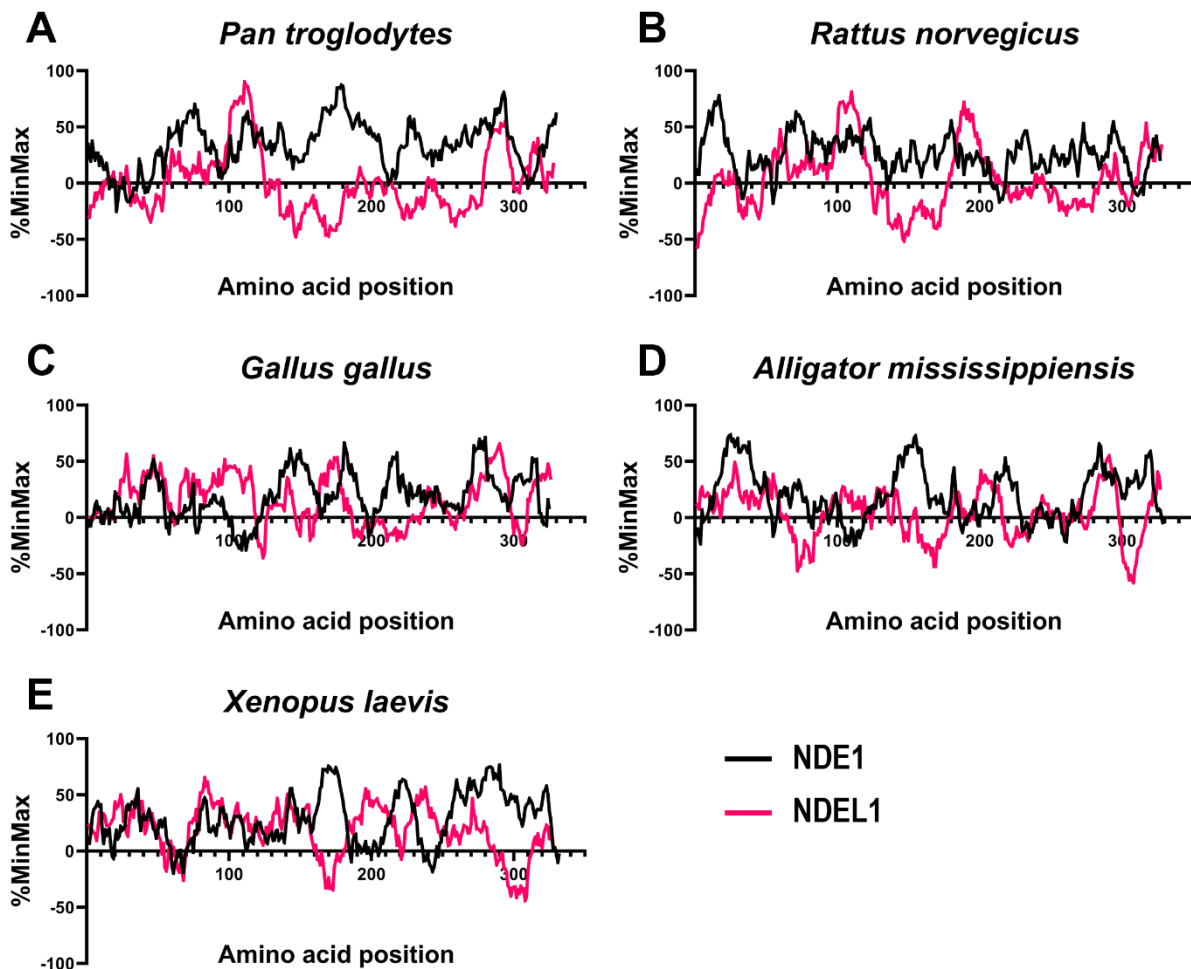
Figure 10. **Pairwise comparison of NDE1 and NDEL1 rare codon usage.** %MinMax value representing codon rarity for each amino acid position in NDE1 and NDEL1, shown from N-terminus to C-terminus. Rare codon usage was calculated using the Clark Lab Rare Codon Calculator (www.codons.org) and the corresponding codon frequency values acquired from the Codon Usage Database (http://www.kazusa.or.jp/codon/) for each representative species (79,82). Comparisons are shown for species representing different vertebrate genera: western lowland gorilla (A), rat (B), chicken (C), American alligator (D) and African clawed frog (E).

To assess the evolutionary conservation of this difference, several other species were analysed. Figure 10 shows how %MinMax values change across both gene sequences in species representing primates, mammals, birds, reptiles, and amphibians. Average values of these results were further analysed by paired t-test, suggesting the increase in NDEL1 rare codon usage is present in all representative species we chose to investigate, except for birds (Figure 11). While the difference was present in zebra finches (*Taeniopygia guttata*), *NDE1* and *NDEL1* genes in chickens (*Gallus gallus*) showed no difference in codon usage rarity.
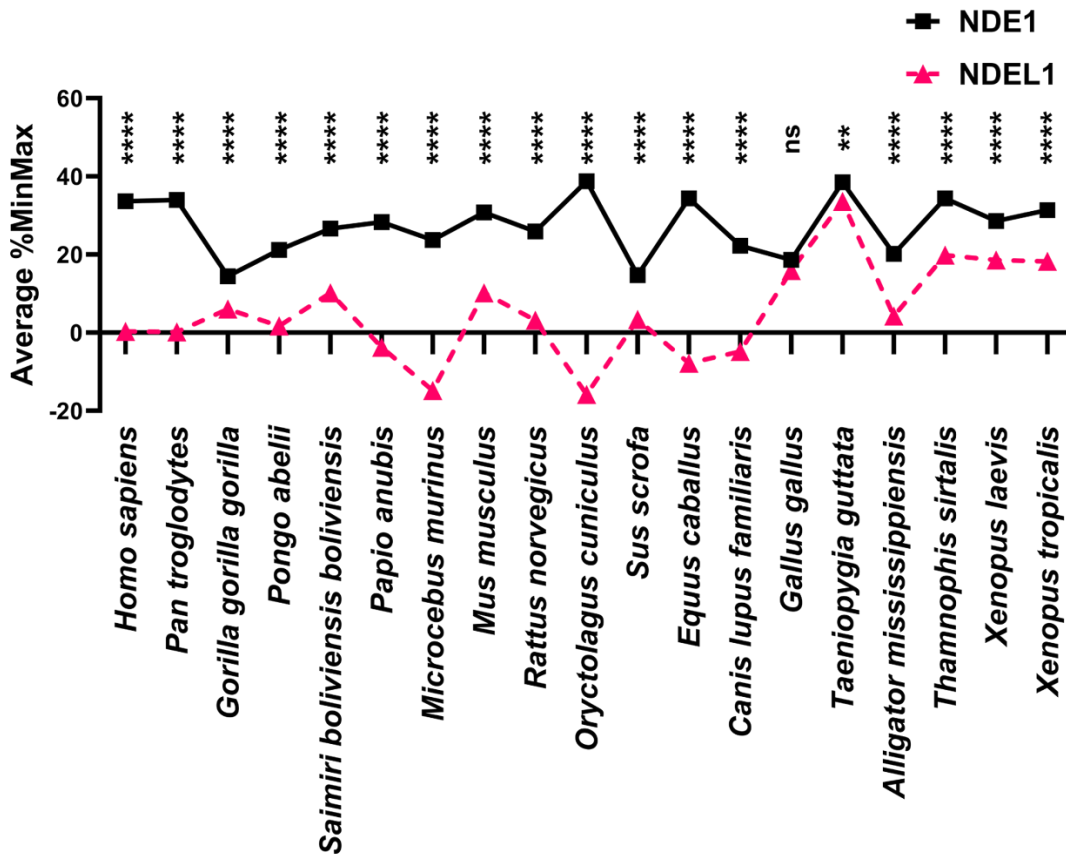
Figure 11. **NDEL1 shows a higher average frequency of rare codon usage compared to NDE1 in multiple vertebrate species.** Lower values of average %MinMax for NDEL1 indicate increased frequency of rare codon usage compared to NDE1 across multiple species. Rare codon usage was calculated using the Clark Lab

Rare Codon Calculator (www.codons.org) (79). Statistical analysis was performed by paired two-tailed t-test (ns, nonsignificant; **p≤0.01; ****p ≤ 0.0001).

Representative species were additionally categorized into non-human primates, non-primate mammals and non-mammalian vertebrates to compare average %MinMax values in grouped vertebrate classifications. As expected, increased *NDEL1* rare codon usage compared to *NDE1* was conserved in non-human primates and non-primate mammals (Figure 12). Interestingly, in this case, non-mammalian vertebrates showed no significant difference between rare codon usage frequencies.
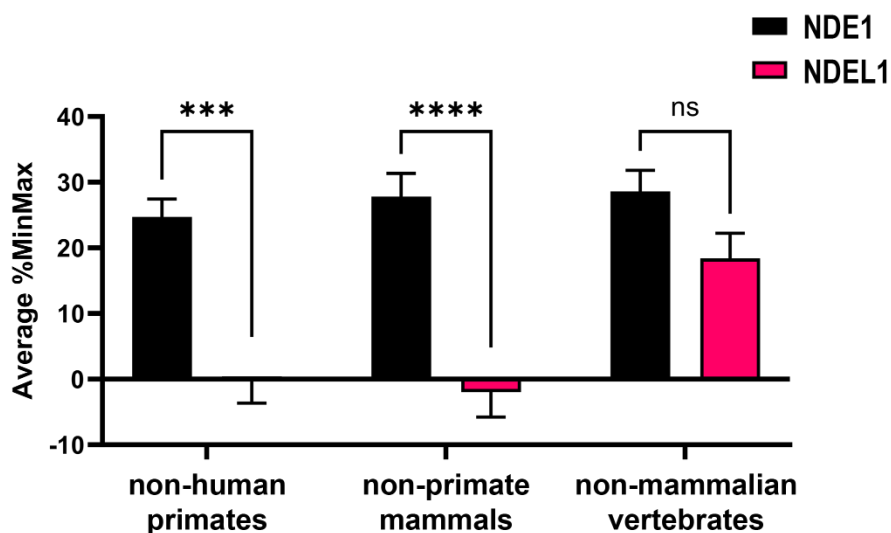
Figure 12. **Rare codon usage is increased in NDEL1 compared to NDE1 in non-human primates and non-primate mammals.** Grouped average %MinMax values for *NDE1* and *NDEL1* codon usage, error bars show SEM. Rare codon usage was calculated using the Clark Lab Rare Codon Calculator (www.codons.org) (79). Statistical analysis was performed by paired two-tailed t-test (ns, nonsignificant; ***p≤0.001; ****p ≤ 0.0001).

4.2. Verification of wild type and switched codon NDE1 and NDEL1 expression by Western blotting

All constructs used in this thesis were first confirmed through sequencing and alignment with known NDE1 and NDEL1 nucleotide and amino acid sequences. Figure 8 shows sequence alignment of both FLAG-tagged wild type and switched codon constructs, and identical results were observed for V5-tagged constructs.

Next, we confirmed proper expression of these constructs in the HEK293 cell line. Transfected cells were lysed, and protein band sizes were analysed by Western blotting. Constructs in pdcDNA-FlagMyc vectors showed bands around 50 kDa, which was slightly higher than the expected bands at 39 kDA and 40 kDa for FLAG-tagged NDE1 and NDEL1, respectively (Figure 13A). Both NDE1 and NDEL1 are known to be highly phosphorylated, which introduces negative charge phosphate groups to the modified proteins. These negative charges can result in an apparent increase in protein size on SDS-PAGE. Equivalent constructs in pMAX vectors showed bands at 44 kDa for NDE1-WT and NDE1-NLc, and at 46 kDa for NDEL1-WT and NDEL1-Nc, which was again slightly higher than expected (Figure 13B). Additionally, there were less intense bands present at approximately 95 kDa for all V5-tagged constructs. This was expected as both NDE1 and NDEL1 are known to form dimers through their long N-terminal coiled-coil domains, making it more challenging to break the interaction between the monomers compared to other protein-protein interactions (8).
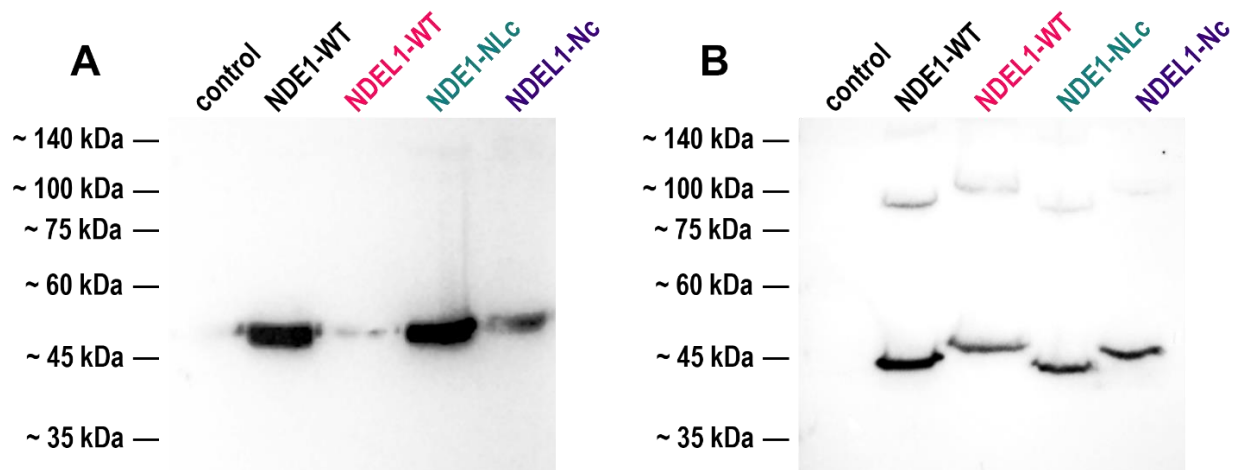
Figure 13. **Western blot analysis of wild type and switched codon NDE1 and NDEL1 proteins expressed in HEK293 cells.** (A) HEK293 cells transfected with constructs in pdcDNA-FlagMyc vectors expressed FLAG-tagged proteins. The membrane was stained with anti-FLAG M2 primary and goat anti-mouse secondary antibody. (B) HEK293 cells transfected with constructs in pMAX vectors expressed V5-tagged proteins. The membrane was stained with anti-V5 primary and goat anti-mouse secondary antibody. Protein bands were visualized using the Pierce ECL Western Blotting Substrate kit and Bio-Rad ChemiDoc Imaging System. Controls included lysates from mock transfected cells. All cells were transfected with 0.5 µg of plasmid DNA.

4.3. NDE1-WT exhibits increased expression levels compared to NDEL1-WT

Given that NDEL1 has a higher frequency of rare codon usage than NDE1, we hypothesized that NDE1-WT will be expressed in HEK293 cells at higher levels than NDEL1-WT when transfected into cells. Furthermore, we transfected cells with switched codon constructs, NDE1-NLc and NDEL1-Nc, to investigate potential variations in their expression compared to wild type proteins. FLAG-tagged constructs were transfected into cells in three biological replicates, each consisting of three technical replicates. The negative controls for each experiment were lysates from mock transfected cells.

When comparing the two wild type proteins, NDE1-WT exhibited increased band intensity over NDEL1-WT (Figure 14A), which is in line with our predictions. Interestingly, we did not observe NDE1 as being more highly expressed than NDEL1 when their codons were switched, suggesting that the rarity of codons is responsible for changes in protein expression. The results also provided a hint that NDE1-NLc might have lower expression than NDEL1-Nc, but the observed difference was not statistically significant. Additionally, one-way ANOVA was performed, but did not reveal any significant differences between band intensities of the four proteins. Analysed FLAG-tagged protein band intensities are shown in Figure 14B and were normalized against β-actin band intensities (also shown on Figure 14B). This normalization helped eliminate potential variations in results due to varying numbers of cells present in each of the lysates.
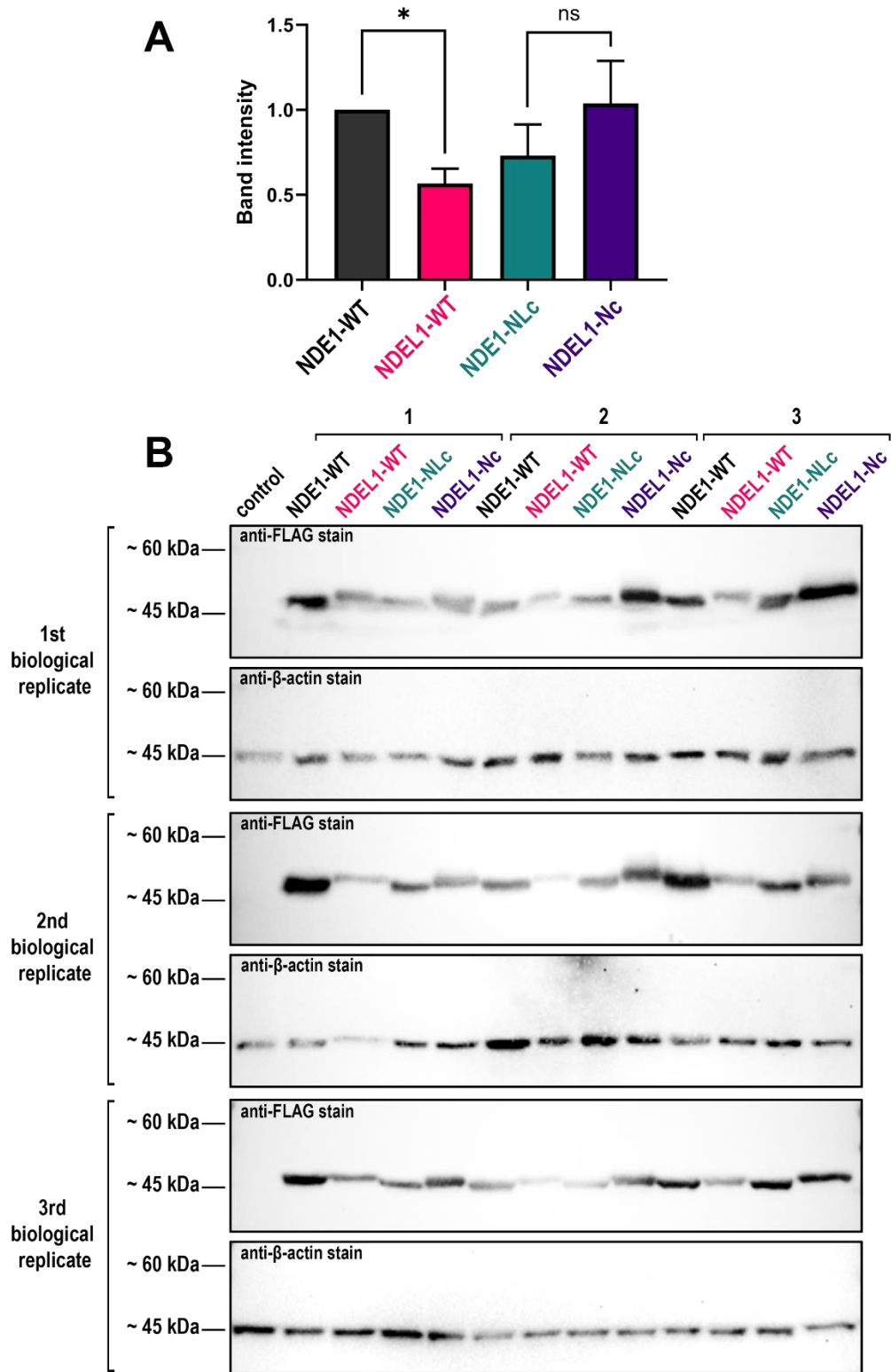
Figure 14. **NDE1 and NDEL1 protein expression in HEK293 cells transfected with wild- type vs. switched codon FLAG-tagged constructs.** (A) Protein band

intensity following Western Blot analysis was normalized with band intensity following anti-β-actin staining. NDE1-WT band intensity was used as a positive control. Average intensities of three replicates were plotted, error bars show SEM. (B) Western blot analysis of three biological replicates of cell transfections stained for NDE1 and NDEL1 proteins. Membranes were stained with anti-FLAG M2 or anti-β-actin primary and goat anti-mouse secondary antibody. Protein bands were visualized using the Pierce ECL Western Blotting Substrate kit and Bio-Rad ChemiDoc Imaging System. Negative controls included lysates from mock transfected cells. All cells were transfected with 0.5 µg of plasmid DNA. Statistical analysis was performed by paired two-tailed t-test (ns, nonsignificant; * $p \leq 0.05$).

Next, we wanted to determine whether the observed results were influenced by the expression system used. To achieve this, we performed an identical experimental setup for V5-tagged constructs as was done with FLAG-tagged constructs. Comparison of wild type proteins revealed NDE1-WT to have higher band intensities than NDEL1-WT, corresponding with the results obtained from FLAG-tagged proteins (Figure 15A). No significant differences were noted between NDE1-NLc and NDEL1-Nc, just like there were no differences in comparing wild type to their respective switched codon pairing. One-way ANOVA was also performed for these results, but no significant differences in band intensities were found.

As previously mentioned, V5-tagged proteins showed two distinct bands, with the one at approximately 95 kDa corresponding to the dimer form (Figure 15B). We decided to include both bands for our analyses to determine total protein values to avoid influencing results by excluding proteins that happened to form dimer units.
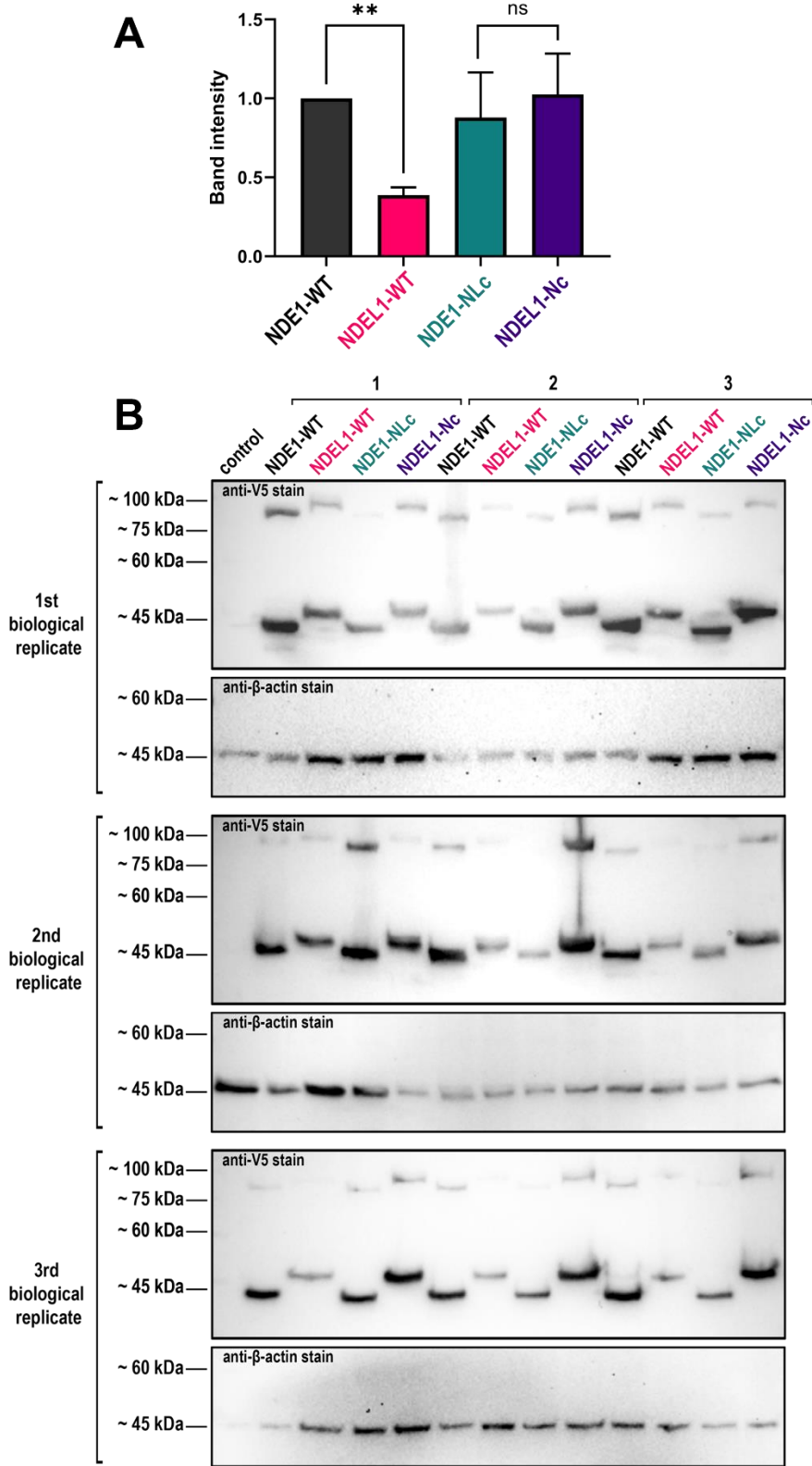
Figure 15. **NDE1 and NDEL1 protein expression in HEK293 cells transfected with wild type vs. switched codon V5-tagged constructs.** Protein band intensity

following Western Blot analysis was normalized with band intensity following anti-β-actin staining. NDE1-WT band intensity was used as a positive control. Average intensities of three replicates were plotted, error bars show SEM. (B) Western blot analysis of three biological replicates of cell transfections stained for NDE1 and NDEL1 proteins. Membranes were stained with anti-V5 or anti-β-actin primary and goat anti-mouse secondary antibody. Protein bands were visualized using the Pierce ECL Western Blotting Substrate kit and Bio-Rad ChemiDoc Imaging System. Negative controls included lysates from mock transfected cells. All cells were transfected with 0.5 µg of plasmid DNA. Statistical analysis was performed by paired two-tailed t-test (ns, nonsignificant; ** $p \leq 0.01$).

4.4. Wild type and switched codon NDE1 and NDEL1 protein expression is localized in cell cytoplasm

Following our Western blotting results, we decided to view HEK293 cells using fluorescent microscopy to assess NDE1 and NDEL1 expression patterns. Successfully expressed FLAG-tagged proteins emitted a bright red fluorescence, while cellular actin is represented by green fluorescence, and cell nuclei emit blue fluorescence (Figure 16). As expected, both wild type and switched NDE1 and NDEL1 were seen to localize in the cell cytoplasm, mainly in the perinuclear area, and were forming filamentous-like structures that likely aligned with the microtubule network within the cells. We did not note any obvious differences in expression patterns between the proteins, and no aggregates were detected. However, due to time constraints, we could not perform a detailed examination.
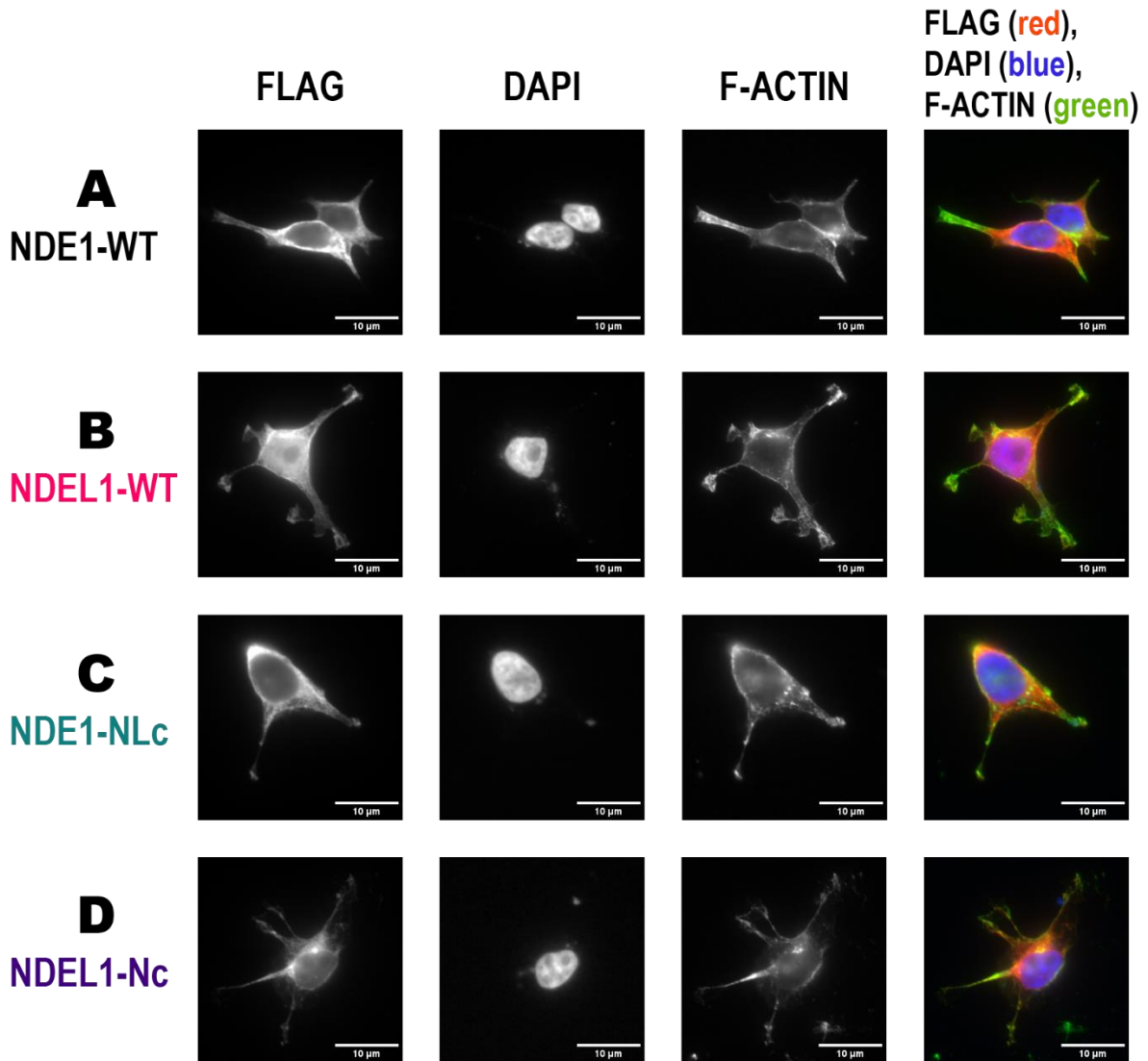
Figure 16. **Fluorescent microscopy of HEK293 cells transfected with wild type and switched codon NDE1 and NDEL1 FLAG-tagged proteins.** Proteins were labelled with primary anti-FLAG M2 and secondary goat anti-mouse 555 nm, shown in red on the figure. Cell nuclei were stained with DAPI (blue), and cellular actin was stained with Phalloidin (green). Images were captured on a fluorescent microscope with CellSense software under 60x magnification. Scale bars represent 10 µm.

5. Discussion

The paralogs NDE1 and NDEL1 have been identified as key components in cell mitosis and neurodevelopment, often acting as interactors with other known proteins including dynein, LIS1, CENP-F and katanin (9,11,20). Despite originating from a gene duplication event and having high amino acid sequence similarity, their nucleic acid sequences show high variability, suggesting examining the potential effect of codon usage bias might allow insight into their differences.

5.1. Exploring NDEL1 increased rare codon usage in humans and multiple mammalian species

In this thesis, we wanted to explore the frequency of rare versus common codon usage frequency in their respective genetic sequences in humans. As expected, pairwise comparison in the frequency of codon rarity spanning the amino acid sequence showed that NDEL1 amino acids are encoded by codons that are considered rare in humans across most of the sequence (Figure 9A). Furthermore, the average values of rare codon usage frequency were significantly lower in *NDEL1* than *NDE1*, suggesting that human *NDEL1* is enriched with rare codons (Figure 9B). This difference may be key to understanding the underlying cause in the functional and expressional differences these proteins exhibit in cells.

Because NDE1 and NDEL1 can be identified as distinctive proteins in vertebrates, we next wanted to examine whether the differential rare codon usage can be seen in other species. For the analysis we chose representative species of major vertebrate genera that had available curated or predicted *NDE1* and *NDEL1* genetic sequences. This analysis did not include fish, as studies in zebrafish showed that an additional gene duplication event occurred, and in addition to NDE1, there are two orthologs of the NDEL1 protein (22). As codon rarity varies among species, each calculation was performed using the respective data corresponding to each organism.

Interestingly, almost all examined representative species showed a similar result as seen in humans, with *NDEL1* having a greater frequency of rare codon usage. The only exception was in chickens, where no difference in used codon rarity was seen. In addition, another species of bird, the zebra finch, showed *NDEL1* having more rare codons, but the difference compared to *NDE1* was not as significant as in other species. We then grouped the representative species into non-human primates, non-primate mammals and non-mammalian vertebrates to compare the rare codon bias in the proteins in major vertebrate genera. Both non-human primates and non-primate mammals showed a significant increase in rare codon usage in *NDEL1* compared to *NDE1*, suggesting the difference in rare codon bias is conserved across mammalian species. It is important to note that when grouped, non-mammalian vertebrates had no significant difference in rare codon bias between the two genes. We suspect that this result is affected by the representative bird species included in the category, as when examined separately, reptiles and amphibians did exhibit a significant difference.

Evolutionary conservation of *NDEL1* having a higher frequency of rare codons compared to *NDE1* highlights the likelihood of rare codon bias playing a crucial role in their functional differences. Moreover, this observation implies that the differences in rare codon bias are not random but rather essential elements that contribute to the functionality of these proteins.

5.2. Switching common and rare codons might influence NDE1 and NDEL1 expression levels in cells

Rare codon usage bias is thought to influence protein translation speed and expression levels (80). We next aimed to examine if NDEL1 enrichment for rare codons might influence its expression levels in a human cell line, specifically in HEK293 cells. To achieve this, four different protein constructs

were used, wild type NDE1 and NDEL1, and switched codon NDE1 and NDEL1. The switched codon NDE1 construct used codons that matched those used in the *NDEL1* gene as closely as possible, while the amino acid sequence remained identical to wild type NDE1. Following the same approach, the switched codon NDEL1 construct was also generated.

To analyse protein expression levels, FLAG-tagged proteins were analysed by Western blotting, and protein band intensity was compared. We hypothesised that in wild type constructs NDE1 would be more expressed than NDEL1, and that the codon switch would produce contrasting results, with NDEL1-Nc being more highly expressed than NDE1-NLc. Results from three biological replicates revealed that NDE1-WT is expressed in higher levels than NDEL1-WT, which we expected (Figure 14A). However, comparison of their switched codon counterparts, NDE1-NLc and NDEL1-Nc revealed the loss of this significant difference in expression. NDE1-NLc showed a slightly lower expression level than NDEL1-Nc, but statistical analysis did not show this result as being significant. The lack of a statistically significant difference in switched codon constructs suggested that, while not completely reversing expression levels of the proteins, used codon rarity did in fact play a role in protein expression levels.

To ensure that our initial findings were not a result of an anomaly caused by the expression system used, three more biological replicates of the same experiments were performed, this time using V5-tagged proteins. In this scenario, similar results were obtained, with NDE1-WT being expressed in significantly higher levels than NDEL1-WT (Figure 15A). Although NDE1-NLc showed a slightly lower expression level than NDEL1-Nc, this difference was again, not significant. While not statistically significant, it is interesting that in both expression systems we noted hints of NDE1-NLc being expressed in lower levels than its NDE1-WT. Similarly, NDEL1-Nc was expressed in higher levels than NDEL1-WT.

Taken together, these results suggest that codon rarity does affect expression levels of NDE1 and NDEL1 proteins, but the codon switch did not show as drastic a change as we expected. It is important to note that our data consisted of only three biological replicates, each containing three technical replicates, but there was a certain degree of variability in band intensity values. In addition, only one cell line, HEK293, was used to conduct the experiments.

5.3. NDE1 and NDEL1 can be seen in similar cellular areas

Lastly, we wanted to examine whether wild type or switched codon NDE1 and NDEL1 show different expression patterns in HEK293 cells examined by cell microscopy. Because of their cellular roles as mediators of the dynein transport pathway and multiple roles during mitosis (8,11,17), we suspected that both proteins would be expressed in filamentous-like structures that seem to follow the cytoskeleton pattern. Furthermore, we wanted to confirm that switching codons did not affect protein localization.

HEK293 cells successfully transfected with NDE1-WT, NDEL1-WT, NDE1-NLc and NDEL1-Nc did not show obvious differences in the cell area where proteins were expressed (Figure 16). They formed a filamentous-like network that seemed to follow the cytoskeleton structure, which is likely a result of the connection between their cellular roles and the microtubule network in cells. Because of the association of the proteins with the centrosome, observing most protein expression in the perinuclear area was expected.

Importantly, no obvious difference was seen between NDE1 and NDEL1 localization in cells transfected with wild type or switched codon constructs, confirming that despite being encoded for by codons considered rare in humans, there was no effect on protein expression. In addition, we examined

all the samples for potential signs of protein aggregation, for which we found no evidence.

However, it's important to note that our results represent preliminary assessment of protein expression within cells, which has several limitations. This assessment was based on a single replicate, and further studies would benefit from multiple replicates to enhance reliability. Additionally, like our analysis of protein expression levels, this experiment utilized only one cell line.

5.4. Further investigation of rare codon bias influence

Despite our results showing promising results, there were major limitations in our experiments, which should be resolved in further studies. During our initial analysis of expression levels in FLAG-tagged proteins, the technical replicates did show a great amount of variability in band intensities, even after normalizing the data with β-actin band values to account for the number of cells in each sample. However, a bigger limitation were the three biological replicates we had, considering that is the minimum required number of experiments needed to be able to draw a conclusion. The variability these showed suggests that in the future, it is necessary to increase the number of biological replicates to confirm our preliminary results. Another possibility includes establishing cell lines with NDE1 or NDEL1 integrated in their genome. These permanently transfected cells could be generated either by viral transfection or the Clustered Regularly Interspaced Short Palindromic Repeats (CRISPR) / CRISPR-associated protein 9 (Cas9) gene editing technology. This method would help mitigate the unpredictability associated with the success rate of transfections.

Although we confirmed our results in another expression system, it was interesting to observe that V5-tagged NDE1-WT, NDEL1-WT, NDE1-NLc and NDEL1-Nc formed both monomers and dimers, while FLAG-tagged proteins

had no dimers present in the samples. Because NDE1 and NDEL1 are known to form dimers and tetramers in solution (8), the cause of the observed difference between the two expression systems remains unknown. Further studies should include other expression systems to investigate the potential cause of variation in the presence of dimeric protein forms. It is important to note that both plasmids used in the thesis have cytomegalovirus (CMV) promoters, which are very highly expressed, potentially masking results. To avoid this, it would be beneficial to generate plasmids in which NDE1 and NDEL1 are expressed under their natural promoters.

Lastly, our observation of expression patterns of wild type and switched codon NDE1 and NDEL1 allowed us to initially compare whether the codon switch influenced where the proteins are localized in cells. Due to the low number of biological replicates, this observation can only serve as a preliminary indication of what could be explored in further studies. In addition, we used HEK293 cells in our experiment, and it would be beneficial to transfect a neuroblastoma cell line for the purpose of fluorescent microscopy. Because of their role in mitosis, it would be interesting to examine cellular localization of NDE1 and NDEL1 in different mitotic stages, which might allow better understanding of their roles.

Furthermore, it's worth emphasizing that this thesis primarily concentrated on exploring the impact of codon rarity on protein expression levels, which may indicate rare codon bias to play a role in NDE1 and NDEL1 functional differences. Future studies performed using the switched codon constructs focused on distinctive NDE1 and NDEL1 functional roles (Figure 5) may show intriguing results. For instance, considering that wild-type NDEL1 is exhibits peptidase activity, it would be intriguing to investigate whether rare codon usage influences this specific function. On a similar note, wild type NDE1 can prevent DNA double stranded breaks and is crucial for S phase progression, but the effect of codon rarity on this function has not yet been studied.

6. Conclusion

In this thesis, we examined if increased frequency of rare codon usage in NDEL1 affects its expression levels in cells compared to NDE1, which shows a preference for more common codons. Rare codon bias, the preferential usage of certain synonymous codons, has been noted in multiple organisms (80). Because of rare codons being associated with slower translation speed and lower expression levels in proteins, we investigated whether codon rarity affects NDE1 and NDEL1 expression levels in HEK293 cells.

Human *NDEL1* exhibits an enrichment in rare codon usage, as opposed to *NDE1* which uses more common codons. We analysed both genes for rare codon bias across multiple species representing major vertebrate genera and found this difference to be conserved in primates and non-primate mammals, indicating these species as potential model organisms for *in vivo* studies on NDE1 and NDEL1.

Our results show that wild type NDE1 exhibits higher expression levels when introduced into cells using the same system and under the same promoter, as opposed to wild-type NDEL1. Furthermore, we observed that this difference in expression is diminished by switching the codons that the proteins are encoded by. This was seen in two different expression systems, suggesting that the effect is not caused by an unknown anomaly. Although the codon switch did not completely reverse expression levels as we hypothesized, the loss of expression level differences suggests that rare codon usage does affect protein levels in cells when it comes to NDE1 and NDEL1. In addition, we showed preliminary evidence that the codon switch did not influence protein localization patterns in transfected cells.

Finally, further studies on how rare codon bias affects human NDE1 and NDEL1 proteins might give valuable insights into the mechanisms that underline the distinct roles observed in various cellular processes.

Financial support

7. Literature

1.   World Health Organization. World mental health report: transforming mental health for all. 2022 Jun 16 [cited 2023 Aug 23]; Available from: https://archive.hshsl.umaryland.edu/handle/10713/20295

2.   Dehbozorgi R, Shahriari M, Fereidooni-Moghadam M, Moghimi-Sarani E. Family-centered collaborative care for patients with chronic mental illness: A systematic review. J Res Med Sci [Internet]. 2023 Jan 1 [cited 2023 Aug 23];28(1):6. Available from: https://pubmed.ncbi.nlm.nih.gov/36974116/

3.   Zumstein N, Riese F. Defining Severe and Persistent Mental Illness—A Pragmatic Utility Concept Analysis. Front Psychiatry. 2020 Jul 6;11:530582.

4.   Chimara M, Van Niekerk L, van Biljon HM. Original research: Scoping review exploring vocational rehabilitation interventions for mental health service users with chronic mental illness in low-income to upper-middle-income countries. BMJ Open [Internet]. 2022 May 9 [cited 2023 Aug 23];12(5):e059211. Available from: /pmc/articles/PMC9086611/

5.   World Health Organization. International Statistical Classification of Diseases and Related Health Problems [Internet]. 11th ed. 2019 [cited 2023 Aug 30]. Available from: https://icd.who.int/en

6.   American Psychiatric Association. Diagnostic and Statistical Manual of Mental Disorders (5th edition). Washington DC: American Psychiatric Publishing; 2013.

7.   Martin J, Taylor MJ, Lichtenstein P. Assessing the evidence for shared genetic risks across psychiatric disorders and traits. Psychol Med [Internet]. 2018 Aug 1 [cited 2023 Aug 23];48(11):1759. Available from: /pmc/articles/PMC6088770/

8. Soares DC, Bradshaw NJ, Zou J, Kennaway CK, Hamilton RS, Chen ZA, et al. The Mitosis and Neurodevelopment Proteins NDE1 and NDEL1 Form Dimers, Tetramers, and Polymers with a Folded Back Structure in Solution. J Biol Chem [Internet]. 2012 Sep 9 [cited 2023 Aug 1];287(39):32381. Available from: /pmc/articles/PMC3463352/

9. Derewenda U, Tarricone C, Choi WC, Cooper DR, Lukasik S, Perrina F, et al. The structure of the coiled-coil domain of Ndel1 and the basis of its interaction with Lis1, the causal protein of Miller-Dieker lissencephaly. Structure [Internet]. 2007 Nov 13 [cited 2023 Aug 2];15(11):1467–81. Available from: https://pubmed.ncbi.nlm.nih.gov/17997972/

10. Pei Z, Lang B, Fragoso YD, Shearer KD, Zhao L, Mccaffery PJA, et al. The expression and roles of Nde1 and Ndel1 in the adult mammalian central nervous system. Neuroscience [Internet]. 2014 Jun 20 [cited 2023 Jun 15];271(100):119–36. Available from: https://pubmed.ncbi.nlm.nih.gov/24785679/

11. Garrott SR, Gillies JP, DeSantis ME. Nde1 and Ndel1: Outstanding Mysteries in Dynein-Mediated Transport. Front Cell Dev Biol [Internet]. 2022 Apr 12 [cited 2023 Jul 10];10. Available from: https://pubmed.ncbi.nlm.nih.gov/35493069/

12. Reimer JM, Desantis ME, Reck-Peterson SL, Leschziner AE. Structures of human dynein in complex with the lissencephaly 1 protein, LIS1. Elife. 2023;12.

13. Alkuraya FS, Cai X, Emery C, Mochida GH, Al-Dosari MS, Felie JM, et al. Human mutations in NDE1 cause extreme microcephaly with lissencephaly. Am J Hum Genet [Internet]. 2011 May 13 [cited 2023 Aug 2];88(5):536–47. Available from: https://www.scholars.northwestern.edu/en/publications/human-mutations-in-nde1-cause-extreme-microcephaly-with-lissencep

14. Johnstone M, Maclean A, Heyrman L, Lenaerts AS, Nordin A, Nilsson LG, et al. Copy Number Variations in DISC1 and DISC1-Interacting Partners in Major Mental Illness. Mol Neuropsychiatry [Internet]. 2015 [cited 2023 Aug 2];1(3):175–90. Available from: https://pubmed.ncbi.nlm.nih.gov/27239468/

15. Tropeano M, Ahn JW, Dobson RJB, Breen G, Rucker J, Dixit A, et al. Male-biased autosomal effect of 16p13.11 copy number variation in neurodevelopmental disorders. PLoS One [Internet]. 2013 Apr 18 [cited 2023 Aug 2];8(4). Available from: https://pubmed.ncbi.nlm.nih.gov/23637818/

16. Paciorkowski AR, Keppler-Noreuil K, Robinson L, Sullivan C, Sajan S, Christian SL, et al. Deletion 16p13.11 uncovers NDE1 mutations on the non-deleted homolog and extends the spectrum of severe microcephaly to include fetal brain disruption. Am J Med Genet A [Internet]. 2013 Jul [cited 2023 Aug 2];161A(7):1523–30. Available from: https://pubmed.ncbi.nlm.nih.gov/23704059/

17. Bradshaw NJ, Hayashi MAF. NDE1 and NDEL1 from genes to (mal)functions: parallel but distinct roles impacting on neurodevelopmental disorders and psychiatric illness. Vol. 74, Cellular and Molecular Life Sciences. Birkhauser Verlag AG; 2017. p. 1191–210.

18. Abdel-Hamid MS, El-Dessouky SH, Ateya MI, Gaafar HM, Abdel-Salam GMH. Phenotypic spectrum of NDE1-related disorders: from microlissencephaly to microhydranencephaly. Am J Med Genet A [Internet]. 2019 Mar 1 [cited 2023 Aug 2];179(3):494–7. Available from: https://pubmed.ncbi.nlm.nih.gov/30637988/

19. Bakircioglu M, Carvalho OP, Khurshid M, Cox JJ, Tuysuz B, Barak T, et al. The Essential Role of Centrosomal NDE1 in Human Cerebral Cortex

Neurogenesis. Am J Hum Genet [Internet]. 2011 May 5 [cited 2023 Aug 2];88(5):523. Available from: /pmc/articles/PMC3146716/

20. Bradshaw NJ, Hennah W, Soares DC. NDE1 and NDEL1: twin neurodevelopmental proteins with similar "nature" but different "nurture." Biomol Concepts [Internet]. 2013 Oct [cited 2023 Aug 2];4(5):447–64. Available from: https://pubmed.ncbi.nlm.nih.gov/24093049/

21. Shmueli A, Segal M, Sapir T, Tsutsumi R, Noritake J, Bar A, et al. Ndel1 palmitoylation: a new mean to regulate cytoplasmic dynein activity. EMBO J [Internet]. 2010 Jan 6 [cited 2023 Aug 10];29(1):107–19. Available from: https://pubmed.ncbi.nlm.nih.gov/19927128/

22. Drerup CM, Ahlgren SC, Morris JA. Expression profiles of ndel1a and ndel1b, two orthologs of the NudE-Like gene, in the zebrafish. Gene Expr Patterns [Internet]. 2007 Jun [cited 2023 Aug 10];7(6):672–9. Available from: https://pubmed.ncbi.nlm.nih.gov/17482883/

23. Kent WJ, Sugnet CW, Furey TS, Roskin KM, Pringle TH, Zahler AM, et al. The Human Genome Browser at UCSC. Genome Res [Internet]. 2002 Jun 1 [cited 2023 Aug 1];12(6):996–1006. Available from: https://genome.cshlp.org/content/12/6/996.full

24. Bateman A, Martin MJ, Orchard S, Magrane M, Ahmad S, Alpi E, et al. UniProt: the Universal Protein Knowledgebase in 2023. Nucleic Acids Res. 2023 Jan 6;51(D1):D523–31.

25. Tamura K, Stecher G, Kumar S. MEGA11: Molecular Evolutionary Genetics Analysis Version 11. Mol Biol Evol. 2021 Jul 1;38(7):3022–7.

26. Madeira F, Pearce M, Tivey ARN, Basutkar P, Lee J, Edbali O, et al. Search and sequence analysis tools services from EMBL-EBI in 2022. Nucleic

Acids Res [Internet]. 2022 Jul 1 [cited 2023 Aug 5];50(W1):W276–9. Available from: https://europepmc.org/articles/PMC9252731

27. Robert X, Gouet P. Deciphering key features in protein structures with the new ENDscript server. Nucleic Acids Res [Internet]. 2014 Jul 1 [cited 2023 Aug 5];42(W1):W320–4. Available from: https://dx.doi.org/10.1093/nar/gku316

28. Grigoryan G, Keating AE. Structural specificity in coiled-coil interactions. Curr Opin Struct Biol [Internet]. 2008 Aug [cited 2023 Aug 10];18(4):477. Available from: /pmc/articles/PMC2567808/

29. Zyłkiewicz E, Kijańska M, Choi WC, Derewenda U, Derewenda ZS, Stukenberg PT. The N-terminal coiled-coil of Ndel1 is a regulated scaffold that recruits LIS1 to dynein. Journal of Cell Biology. 2011 Feb 7;192(3):433–45.

30. Feng Y, Olson EC, Stukenberg PT, Flanagan LA, Kirschner MW, Walsh CA. LIS1 regulates CNS lamination by interacting with mNudE, a central component of the centrosome. Neuron [Internet]. 2000 Dec 1 [cited 2023 Aug 15];28(3):665–79. Available from: http://www.cell.com/article/S0896627300001458/fulltext

31. Ye F, Kang E, Yu C, Qian X, Jacob F, Yu C, et al. DISC1 Regulates Neurogenesis via Modulating Kinetochore Attachment of Ndel1/Nde1 during Mitosis. Neuron. 2017 Dec 6;96(5):1041-1054.e5.

32. Soukoulis V, Reddy S, Pooley RD, Feng Y, Walsh CA, Bader DM. Cytoplasmic LEK1 is a regulator of microtubule function through its interaction with the LIS1 pathway. Proc Natl Acad Sci U S A [Internet]. 2005 Jun 14 [cited 2023 Aug 16];102(24):8549–54. Available from: https://www.pnas.org/doi/abs/10.1073/pnas.0502303102

33. Wang S, Zheng Y. Identification of a novel dynein binding domain in nudel essential for spindle pole organization in Xenopus egg extract. J Biol Chem [Internet]. 2011 Jan 7 [cited 2023 Aug 15];286(1):587–93. Available from: https://pubmed.ncbi.nlm.nih.gov/21056974/

34. Nguyen MD, Shu T, Sanada K, Larivière RC, Tseng HC, Park SK, et al. A NUDEL-dependent mechanism of neurofilament assembly regulates the integrity of CNS neurons. Nat Cell Biol [Internet]. 2004 Jul [cited 2023 Aug 16];6(7):595–608. Available from: https://pubmed.ncbi.nlm.nih.gov/15208636/

35. Hu WF, Pomp O, Ben-Omran T, Kodani A, Henke K, Mochida GH, et al. Katanin p80 regulates human cortical development by limiting centriole and cilia number. Neuron [Internet]. 2014 Dec 1 [cited 2023 Aug 16];84(6):1240–57. Available from: https://pubmed.ncbi.nlm.nih.gov/25521379/

36. Toyo-Oka K, Sasaki S, Yano Y, Mori D, Kobayashi T, Toyoshima YY, et al. Recruitment of katanin p60 by phosphorylated NDEL1, an LIS1 interacting protein, is essential for mitotic cell division and neuronal migration. Hum Mol Genet [Internet]. 2005 Nov [cited 2023 Aug 15];14(21):3113–28. Available from: https://pubmed.ncbi.nlm.nih.gov/16203747/

37. Vergnolle MAS, Taylor SS. Cenp-F Links Kinetochores to Ndel1/Nde1/Lis1/Dynein Microtubule Motor Complexes. Current Biology. 2007 Jul 3;17(13):1173–9.

38. Jumper J, Evans R, Pritzel A, Green T, Figurnov M, Ronneberger O, et al. Highly accurate protein structure prediction with AlphaFold. Nature 2021 596:7873 [Internet]. 2021 Jul 15 [cited 2023 Aug 10];596(7873):583–9. Available from: https://www.nature.com/articles/s41586-021-03819-2

39. Varadi M, Anyango S, Deshpande M, Nair S, Natassia C, Yordanova G, et al. AlphaFold Protein Structure Database: massively expanding the structural coverage of protein-sequence space with high-accuracy models. Nucleic Acids Res [Internet]. 2022 Jan 7 [cited 2023 Aug 10];50(D1):D439–44. Available from: https://dx.doi.org/10.1093/nar/gkab1061

40. Pettersen EF, Goddard TD, Huang CC, Couch GS, Greenblatt DM, Meng EC, et al. UCSF Chimera--a visualization system for exploratory research and analysis. J Comput Chem [Internet]. 2004 Oct [cited 2023 Aug 5];25(13):1605–12. Available from: https://pubmed.ncbi.nlm.nih.gov/15264254/

41. Bradshaw NJ, Ogawa F, Antolin-Fontes B, Chubb JE, Carlyle BC, Christie S, et al. DISC1, PDE4B, and NDE1 at the centrosome and synapse. Biochem Biophys Res Commun [Internet]. 2008 Dec 26 [cited 2023 Aug 10];377(4):1091–6. Available from: https://pubmed.ncbi.nlm.nih.gov/18983980/

42. Bradshaw NJ, Soares DC, Carlyle BC, Ogawa F, Davidson-Smith H, Christie S, et al. PKA phosphorylation of NDE1 is DISC1/PDE4 dependent and modulates its interaction with LIS1 and NDEL1. J Neurosci [Internet]. 2011 Jun 15 [cited 2023 Aug 19];31(24):9043–54. Available from: https://pubmed.ncbi.nlm.nih.gov/21677187/

43. Reiner O, Sapir T. LIS1 functions in normal development and disease. Curr Opin Neurobiol [Internet]. 2013 Dec [cited 2023 Aug 16];23(6):951–6. Available from: https://pubmed.ncbi.nlm.nih.gov/23973156/

44. Moon HM, Wynshaw-Boris A. Cytoskeleton in action: lissencephaly, a neuronal migration disorder. Wiley Interdiscip Rev Dev Biol [Internet].

2013 Mar [cited 2023 Aug 16];2(2):229–45. Available from: https://pubmed.ncbi.nlm.nih.gov/23495356/

45. Reiner O, Carrozzo R, Shen Y, Wehnert M, Faustinella F, Dobyns WB, et al. Isolation of a Miller-Dieker lissencephaly gene containing G protein beta-subunit-like repeats. Nature [Internet]. 1993 [cited 2023 Aug 16];364(6439):717–21. Available from: https://pubmed.ncbi.nlm.nih.gov/8355785/

46. Mochida GH. Genetics and biology of microcephaly and lissencephaly. Semin Pediatr Neurol [Internet]. 2009 Sep [cited 2023 Aug 17];16(3):120. Available from: /pmc/articles/PMC3565221/

47. Juric-Sekhar G, Hevner RF. Malformations of Cerebral Cortex Development: Molecules and Mechanisms. Annu Rev Pathol [Internet]. 2019 [cited 2023 Aug 17];14:293–318. Available from: https://pubmed.ncbi.nlm.nih.gov/30677308/

48. Di Donato N, Chiari S, Mirzaa GM, Aldinger K, Parrini E, Olds C, et al. Lissencephaly: Expanded imaging and clinical classification. Am J Med Genet A [Internet]. 2017 Jun 1 [cited 2023 Aug 17];173(6):1473–88. Available from: https://pubmed.ncbi.nlm.nih.gov/28440899/

49. Fry AE, Cushion TD, Pilz DT. The genetics of lissencephaly. Am J Med Genet C Semin Med Genet [Internet]. 2014 [cited 2023 Aug 17];166C(2):198–210. Available from: https://pubmed.ncbi.nlm.nih.gov/24862549/

50. Girdler SJ, Confino JE, Woesner ME. Exercise as a Treatment for Schizophrenia: A Review. Psychopharmacol Bull [Internet]. 2019 Feb 2 [cited 2023 Aug 17];49(1):56. Available from: /pmc/articles/PMC6386427/

51. Saha S, Chant D, Welham J, McGrath J. A Systematic Review of the Prevalence of Schizophrenia. PLoS Med [Internet]. 2005 [cited 2023 Aug 17];2(5):e141. Available from: https://journals.plos.org/plosmedicine/article?id=10.1371/journal.pmed.0020141

52. McCutcheon RA, Reis Marques T, Howes OD. Schizophrenia-An Overview. JAMA Psychiatry [Internet]. 2020 Feb 1 [cited 2023 Aug 17];77(2):201–10. Available from: https://pubmed.ncbi.nlm.nih.gov/31664453/

53. Burdick KE, Kamiya A, Hodgkinson CA, Lencz T, Derosse P, Ishizuka K, et al. Elucidating the relationship between DISC1, NDEL1 and NDE1 and the risk for schizophrenia: evidence of epistasis and competitive binding. Hum Mol Genet [Internet]. 2008 Aug [cited 2023 Jun 15];17(16):2462–73. Available from: https://pubmed.ncbi.nlm.nih.gov/18469341/

54. Kimura H, Tsuboi D, Wang C, Kushima I, Koide T, Ikeda M, et al. Identification of Rare, Single-Nucleotide Mutations in NDE1 and Their Contributions to Schizophrenia Susceptibility. Schizophr Bull [Internet]. 2015 May 1 [cited 2023 Aug 18];41(3):744–53. Available from: https://pubmed.ncbi.nlm.nih.gov/25332407/

55. Hennah W, Tomppo L, Hiekkalinna T, Palo OM, Kilpinen H, Ekelund J, et al. Families with the risk allele of DISC1 reveal a link between schizophrenia and another component of the same molecular pathway, NDE1. Hum Mol Genet [Internet]. 2007 Mar 1 [cited 2023 Aug 18];16(5):453–62. Available from: https://pubmed.ncbi.nlm.nih.gov/17185386/

56. She ZY, Yang WX. Molecular mechanisms of kinesin-14 motors in spindle assembly and chromosome segregation. J Cell Sci [Internet]. 2017 Jul 1 [cited 2023 Aug 13];130(13):2097–110. Available from: https://pubmed.ncbi.nlm.nih.gov/28668932/

57. Kardon JR, Vale RD. Regulators of the cytoplasmic dynein motor. Nat Rev Mol Cell Biol [Internet]. 2009 Dec [cited 2023 Aug 13];10(12):854–65. Available from: https://pubmed.ncbi.nlm.nih.gov/19935668/

58. Canty JT, Tan R, Kusakci E, Fernandes J, Yildiz A. Structure and Mechanics of Dynein Motors. Annu Rev Biophys [Internet]. 2021 May 6 [cited 2023 Aug 19];50:549–74. Available from: https://pubmed.ncbi.nlm.nih.gov/33957056/

59. King SM. AAA domains and organization of the dynein motor unit. J Cell Sci [Internet]. 2000 [cited 2023 Aug 19];113 (Pt 14)(14):2521–6. Available from: https://pubmed.ncbi.nlm.nih.gov/10862709/

60. Carter AP, Diamant AG, Urnavicius L. How dynein and dynactin transport cargos: a structural perspective. Curr Opin Struct Biol. 2016 Apr 1;37:62–70.

61. Zhang K, Foster HE, Rondelet A, Lacey SE, Bahi-Buisson N, Bird AW, et al. Cryo-EM Reveals How Human Cytoplasmic Dynein Is Auto-inhibited and Activated. Cell [Internet]. 2017 Jun 15 [cited 2023 Aug 19];169(7):1303-1314.e18. Available from: https://pubmed.ncbi.nlm.nih.gov/28602352/

62. Reck-Peterson SL, Redwine WB, Vale RD, Carter AP. The cytoplasmic dynein transport machinery and its many cargoes. Nature Reviews Molecular Cell Biology 2018 19:6 [Internet]. 2018 Apr 16 [cited 2023 Aug 19];19(6):382–98. Available from: https://www.nature.com/articles/s41580-018-0004-3

63. Cianfrocco MA, Desantis ME, Leschziner AE, Reck-Peterson SL. Mechanism and regulation of cytoplasmic dynein. Annu Rev Cell Dev Biol [Internet]. 2015 Nov 13 [cited 2023 Aug 19];31:83–108. Available from: https://pubmed.ncbi.nlm.nih.gov/26436706/

64. McKenney RJ, Vershinin M, Kunwar A, Vallee RB, Gross SP. LIS1 and NudE induce a persistent dynein force-producing state. Cell [Internet]. 2010 [cited 2023 Aug 19];141(2):304–14. Available from: https://pubmed.ncbi.nlm.nih.gov/20403325/

65. McKenney RJ, Weil SJ, Scherer J, Vallee RB. Mutually exclusive cytoplasmic dynein regulation by NudE-Lis1 and dynactin. J Biol Chem [Internet]. 2011 Nov 11 [cited 2023 Aug 19];286(45):39615–22. Available from: https://pubmed.ncbi.nlm.nih.gov/21911489/

66. Liang Y, Yu W, Li Y, Yu L, Zhang Q, Wang F, et al. Nudel modulates kinetochore association and function of cytoplasmic dynein in M phase. Mol Biol Cell [Internet]. 2007 Jul [cited 2023 Aug 20];18(7):2656–66. Available from: https://pubmed.ncbi.nlm.nih.gov/17494871/

67. Stehman SA, Chen Y, McKenney RJ, Vallee RB. NudE and NudEL are required for mitotic progression and are involved in dynein recruitment to kinetochores. J Cell Biol [Internet]. 2007 Aug 8 [cited 2023 Aug 20];178(4):583. Available from: /pmc/articles/PMC2064466/

68. Bolhy S, Bouhlel I, Dultz E, Nayak T, Zuccolo M, Gatti X, et al. A Nup133-dependent NPC-anchored network tethers centrosomes to the nuclear envelope in prophase. J Cell Biol [Internet]. 2011 Mar 3 [cited 2023 Aug 20];192(5):855. Available from: /pmc/articles/PMC3051818/

69. Gaetani L, Blennow K, Calabresi P, Di Filippo M, Parnetti L, Zetterberg H. Neurofilament light chain as a biomarker in neurological disorders. J Neurol Neurosurg Psychiatry [Internet]. 2019 [cited 2023 Aug 21];90(8). Available from: https://pubmed.ncbi.nlm.nih.gov/30967444/

70. Yuan A, Rao M V., Veeranna, Nixon RA. Neurofilaments and Neurofilament Proteins in Health and Disease. Cold Spring Harb Perspect Biol [Internet].

2017 Apr 1 [cited 2023 Aug 21];9(4). Available from: https://pubmed.ncbi.nlm.nih.gov/28373358/

71. Lynn NA, Martinez E, Nguyen H, Torres JZ. The Mammalian Family of Katanin Microtubule-Severing Enzymes. Front Cell Dev Biol [Internet]. 2021 Aug 3 [cited 2023 Aug 21];9. Available from: https://pubmed.ncbi.nlm.nih.gov/34414183/

72. McNally KP, Bazirgan OA, McNally FJ. Two domains of p80 katanin regulate microtubule severing and spindle pole targeting by p60 katanin. J Cell Sci [Internet]. 2000 [cited 2023 Aug 21];113 (Pt 9)(9):1623–33. Available from: https://pubmed.ncbi.nlm.nih.gov/10751153/

73. Guerreiro JR, Winnischofer SMB, Bastos MF, Portaro FCV, Sogayar MC, De Camargo ACM, et al. Cloning and characterization of the human and rabbit NUDEL-oligopeptidase promoters and their negative regulation. Biochim Biophys Acta [Internet]. 2005 Jul 25 [cited 2023 Aug 31];1730(1):77–84. Available from: https://pubmed.ncbi.nlm.nih.gov/16005531/

74. Hayashi MAF, Portaro FCV, Bastos MF, Guerreiro JR, Oliveira V, Gorrão SS, et al. Inhibition of NUDEL (nuclear distribution element-like)-oligopeptidase activity by disrupted-in-schizophrenia 1. Proc Natl Acad Sci U S A [Internet]. 2005 Mar 8 [cited 2023 Aug 31];102(10):3828–33. Available from: https://pubmed.ncbi.nlm.nih.gov/15728732/

75. Nani J V., Fonseca MC, Engi SA, Perillo MG, Dias CSB, Gazarini ML, et al. Decreased nuclear distribution nudE-like 1 enzyme activity in an animal model with dysfunctional disrupted-in-schizophrenia 1 signaling featuring aberrant neurodevelopment and amphetamine-supersensitivity. J Psychopharmacol [Internet]. 2020 Apr 1 [cited 2023 Aug 31];34(4):467–77. Available from: https://pubmed.ncbi.nlm.nih.gov/31916893/

76. Houlihan SL, Feng Y. The scaffold protein Nde1 safeguards the brain genome during S phase of early neural progenitor differentiation. Elife [Internet]. 2014 [cited 2023 Sep 1];3:e03297. Available from: /pmc/articles/PMC4170211/

77. Chomiak AA, Guo Y, Kopsidas CA, McDaniel DP, Lowe CC, Pan H, et al. Nde1 is required for heterochromatin compaction and stability in neocortical neurons. iScience [Internet]. 2022 Jun 6 [cited 2023 Sep 1];25(6). Available from: /pmc/articles/PMC9121328/

78. Chaney JL, Clark PL. Roles for Synonymous Codon Usage in Protein Biogenesis. Annu Rev Biophys [Internet]. 2015 Jun 22 [cited 2023 Aug 1];44:143–66. Available from: https://pubmed.ncbi.nlm.nih.gov/25747594/

79. Clarke IV TF, Clark PL. Rare Codons Cluster. PLoS One [Internet]. 2008 Oct 15 [cited 2023 Aug 1];3(10):e3412. Available from: https://journals.plos.org/plosone/article?id=10.1371/journal.pone.0003412

80. Liu Y. A code within the genetic code: Codon usage regulates co-translational protein folding. Cell Communication and Signaling [Internet]. 2020 Sep 9 [cited 2023 Aug 22];18(1):1–9. Available from: https://biosignaling.biomedcentral.com/articles/10.1186/s12964-020-00642-6

81. Sánchez R, Grau R, Morgado E. A novel Lie algebra of the genetic code over the Galois field of four DNA bases. Math Biosci. 2006 Jul;202(1):156–74.

82. Nakamura Y, Gojobori T, Ikemura T. Codon usage tabulated from international DNA sequence databases: status for the year 2000. Nucleic

Acids Res [Internet]. 2000 Jan 1 [cited 2023 Aug 1];28(1):292. Available from: https://pubmed.ncbi.nlm.nih.gov/10592250/

83. Atkins JF, Baranov P V. The Distinction Between Recoding and Codon Reassignment. Genetics [Internet]. 2010 Aug [cited 2023 Aug 31];185(4):1535. Available from: /pmc/articles/PMC2921827/

84. Walsh IM, Bowman MA, Soto Santarriaga IF, Rodriguez A, Clark PL. Synonymous codon substitutions perturb cotranslational protein folding in vivo and impair cell fitness. Proc Natl Acad Sci U S A [Internet]. 2020 Feb 18 [cited 2023 Aug 31];117(7):3528–34. Available from: https://www.pnas.org/doi/abs/10.1073/pnas.1907126117

85. Tamura K, Stecher G, Kumar S. MEGA11: Molecular Evolutionary Genetics Analysis Version 11. Mol Biol Evol [Internet]. 2021 Jun 25 [cited 2023 Aug 31];38(7):3022–7. Available from: https://dx.doi.org/10.1093/molbev/msab120

8. List of figures

9. List of tables